

MASTERARBEIT IN PHYSIK

Quantum Error Correction with the GKP Code and Concatenation with Stabilizer Codes

von

Yang Wang

Rheinisch-Westfälisch Technische Hochschule Aachen
Fakultät für Mathematik, Informatik und Naturwissenschaften

07. December 2017

angefertigt am

JARA-Institut für Quanteninformation

vorgelegt bei

Prof. Dr. rer. nat. Barbara M. Terhal

Eidesstattliche Erklärung

Ich versichere, dass

die von mir eingereichte Arbeit *“Quantum Error Correction with the GKP code and Concatenation with Stabilizer Codes”* meine eigene Arbeit ist.

Ich habe keine

sonstigen

Angaben

gemacht.

Am 07.02.2017

(NV)

Acknowledgement

Firstly, I would like to thank my supervisor, Dr. [Name], for his guidance and support throughout the project. I also thank my colleagues and friends for their assistance and encouragement. Finally, I thank my family for their love and support.

Contents

Contents	ii
1 Introduction	1
2 Theoretical Background	3
2.1 QCS	3
2.2 IS	6
2.3 ISLIS	7
2.4 SH	10
3 Quantum Computation with GKP Code States	15
3.1 ISLIS	15
3.2 IS	17
3.3 IS	19
3.4 ISLIS	22
4 Quantum Error Correction with continuous information	25
4.1 ISLIS	26
4.2 ISLIS	31
4.3 ISLIS	36
4.4 ISLIS	37
4.5 ISLIS	45
4.6 ISLIS	46
5 Conclusion and Outlook	49
Bibliography	1

Introduction

The first part of the book is devoted to the study of the properties of the function $f(x) = \frac{1}{x}$. We shall see that this function is harmonic in the sense that it satisfies Laplace's equation in the plane. This property is closely related to the fact that the function $f(x) = \frac{1}{x}$ is the real part of the complex function $F(z) = \frac{1}{z}$.

In the second part of the book we shall study the properties of the function $f(x) = \frac{1}{x^2}$. We shall see that this function is also harmonic in the plane. This property is closely related to the fact that the function $f(x) = \frac{1}{x^2}$ is the real part of the complex function $F(z) = \frac{1}{z^2}$.

The third part of the book is devoted to the study of the properties of the function $f(x) = \frac{1}{x^3}$. We shall see that this function is also harmonic in the plane. This property is closely related to the fact that the function $f(x) = \frac{1}{x^3}$ is the real part of the complex function $F(z) = \frac{1}{z^3}$.

The fourth part of the book is devoted to the study of the properties of the function $f(x) = \frac{1}{x^4}$. We shall see that this function is also harmonic in the plane. This property is closely related to the fact that the function $f(x) = \frac{1}{x^4}$ is the real part of the complex function $F(z) = \frac{1}{z^4}$.

et al. [1]

$$\frac{\sqrt{\pi}}{6} \approx 0.2618$$

Theoretical Background

§2.1
 §2.2
 §2.3
 §2.4

2.1 Ideal GKP Code States

et al. § Ideal GKP Code States

$$\begin{aligned}\hat{q} &= \frac{1}{\sqrt{2}}(\hat{a} + \hat{a}^\dagger), \\ \hat{p} &= \frac{i}{\sqrt{2}}(\hat{a} - \hat{a}^\dagger),\end{aligned}\tag{2.1}$$

\hat{a} and \hat{a}^\dagger

$$[\hat{q}, \hat{p}] = i.\tag{2.2}$$

Each

$|q\rangle$ and $|p\rangle$:

$$\begin{aligned}\hat{q}|q\rangle &= q|q\rangle, \\ \hat{p}|p\rangle &= p|p\rangle,\end{aligned}\tag{2.3}$$

q, p

$$|q\rangle = \int \frac{dp}{\sqrt{2\pi}} e^{ipq} |p\rangle.\tag{2.4}$$

\hat{p} and \hat{q} are the momentum and position operators, respectively, satisfying the canonical commutation relation

$$\begin{aligned}
 |q + u\rangle &= e^{-iu\hat{p}} |q\rangle, \\
 |p + v\rangle &= e^{+iv\hat{q}} |p\rangle,
 \end{aligned}
 \tag{2.5}$$

where u, v are real numbers. From (2.2), one can

2.1.1 Encoding a Qubit into a Harmonic oscillator

In this section, we consider a harmonic oscillator with mass m and frequency ω . The position and momentum operators are

$$\hat{S}_q = e^{-i2\sqrt{\pi}\hat{p}}, \quad \hat{S}_p = e^{i2\sqrt{\pi}\hat{q}}.
 \tag{2.6}$$

We can show that

$$e^A e^B = e^B e^A e^{[A,B]},$$

$$[\hat{S}_q, \hat{S}_p] = 0.$$

We can show that \hat{S}_q and \hat{S}_p are involutions, i.e., $\hat{S}_q^2 = \hat{S}_p^2 = \mathbb{I}$. This implies that \hat{S}_q and \hat{S}_p are Hermitian operators.

$$q, p \in \mathbb{R} \quad \text{and} \quad \sqrt{\pi} = n\sqrt{\pi}, \quad n \in \mathbb{Z}.$$

We define the states $|\bar{0}\rangle$ and $|\bar{1}\rangle$ as

$$\begin{aligned}
 |\bar{0}\rangle &= \sum_n \delta(q - 2n\sqrt{\pi}) |q\rangle = \sum_n |q = 2n\sqrt{\pi}\rangle, \\
 |\bar{1}\rangle &= \sum_n \delta(q - (2n+1)\sqrt{\pi}) |q\rangle = \sum_n |q = (2n+1)\sqrt{\pi}\rangle.
 \end{aligned}
 \tag{2.7}$$

We can show that $|\bar{0}\rangle$ and $|\bar{1}\rangle$ are orthogonal states. We define the operator \bar{X} as

$$\bar{X} = e^{-i\sqrt{\pi}\hat{p}}.$$

We can show that $\bar{X}^2 = \hat{S}_q$. We define the states $|\bar{+}\rangle$ and $|\bar{-}\rangle$ as

$$\begin{aligned}
 |\bar{+}\rangle &= \sum_n \delta(p - 2n\sqrt{\pi}) |p\rangle = \sum_n |p = 2n\sqrt{\pi}\rangle, \\
 |\bar{-}\rangle &= \sum_n \delta(p - (2n+1)\sqrt{\pi}) |p\rangle = \sum_n |p = (2n+1)\sqrt{\pi}\rangle,
 \end{aligned}
 \tag{2.8}$$

and the operator \bar{Z} as

$$\bar{Z} = e^{+i\sqrt{\pi}\hat{q}} = \hat{S}_p^{\frac{1}{2}}.$$

Equation (2.4) can be

rewritten as $\sum_{n=-\infty}^{\infty} \delta(x - nT) = \sum_{n=-\infty}^{\infty} \frac{1}{T} e^{i2\pi \frac{k}{T} x}$, which

$$\begin{aligned} |\bar{0}\rangle &= \sum_n \delta(q - 2n\sqrt{\pi}) |q\rangle = \int \frac{dp}{\sqrt{2\pi}} \sum_n e^{ip2n\sqrt{\pi}} |p\rangle \\ &= \frac{1}{\sqrt{2}} \sum_n \delta(p - n\sqrt{\pi}) |p\rangle \\ &= \frac{1}{\sqrt{2}} (|+\rangle + |-\rangle). \end{aligned} \tag{2.9}$$

Similarly

$$\begin{aligned} |\bar{1}\rangle &= \frac{1}{\sqrt{2}} (|+\rangle + |-\rangle) \propto \sum_n (-1)^n \delta(p - n\sqrt{\pi}) |p\rangle \\ |+\rangle &= \frac{1}{\sqrt{2}} (|+\rangle + |-\rangle) \propto \sum_n \delta(q - n\sqrt{\pi}) |q\rangle \\ |-\rangle &= \frac{1}{\sqrt{2}} (|+\rangle + |-\rangle) \propto \sum_n (-1)^n \delta(q - n\sqrt{\pi}) |q\rangle. \end{aligned}$$

Therefore, we can

write the operators \hat{q} and \hat{p} in terms of the modes

as follows [1, 2, 3, 4]

in *et al.*

2.1.2 Resistance to Small Shift Errors

Consider the state

defined by

$$|\bar{\psi}\rangle = \alpha |\bar{0}\rangle + \beta |\bar{1}\rangle,$$

where

$$|\bar{0}\rangle = \frac{1}{\sqrt{2}} (|+\rangle + |-\rangle)$$

and

$$|\bar{1}\rangle = \frac{1}{\sqrt{2}} (|+\rangle - |-\rangle).$$

$$\hat{S}_q = \exp(i\hat{q}u)$$

$$\hat{S}_p = \exp(-i\hat{p}u)$$

$$\hat{S}_q = \exp(i\hat{q}u)$$

$$\hat{S}_p = \exp(-i\hat{p}u)$$

$$\hat{S}_q = \exp(i\hat{q}u)$$

$$\hat{S}_p = \exp(-i\hat{p}u)$$

$$\begin{aligned} \hat{S}_q e^{-i\hat{p}u} |\bar{\psi}\rangle &= e^{i2\sqrt{\pi}\hat{q}} e^{-i\hat{p}u} |\bar{\psi}\rangle = e^{-i\hat{p}u} e^{i2\sqrt{\pi}\hat{q}} e^{2\sqrt{\pi}u[\hat{q},\hat{p}]} |\bar{\psi}\rangle \\ &= e^{i2\sqrt{\pi}u} e^{-i\hat{p}u} |\bar{\psi}\rangle \end{aligned}$$

where $[A, B] = AB - BA$.

Using

we find

that

$$\hat{S}_q e^{-i\hat{p}u} |\bar{\psi}\rangle = e^{i2\sqrt{\pi}u} e^{-i\hat{p}u} |\bar{\psi}\rangle$$

and

$$\hat{S}_p e^{-i\hat{q}u} |\bar{\psi}\rangle = e^{-i2\sqrt{\pi}u} e^{-i\hat{q}u} |\bar{\psi}\rangle$$

Therefore

$$\hat{S}_q \hat{S}_p e^{-i\hat{p}u} e^{-i\hat{q}u} |\bar{\psi}\rangle = e^{i2\sqrt{\pi}u} e^{-i2\sqrt{\pi}u} e^{-i\hat{p}u} e^{-i\hat{q}u} |\bar{\psi}\rangle = e^{-i\hat{p}u} e^{-i\hat{q}u} |\bar{\psi}\rangle$$

which

$$|\bar{\psi}\rangle = e^{-i\hat{p}u} e^{-i\hat{q}u} |\bar{\psi}\rangle \tag{3.1.2}$$

Therefore

we have

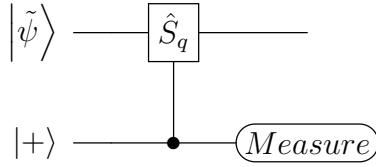


Figure 2.1: Circuit of Controlled- \hat{S}_q gate. where $|\tilde{\psi}\rangle$ is an ideal GKP code state subjected to shift error in the \hat{q} quadrature. The controlled- \hat{S}_q consists of two CNOT gates, it is controlled by the ancilla qubit in state $|+\rangle$. Measure the ancilla qubit in basis $\{|+\rangle, |-\rangle\}$.

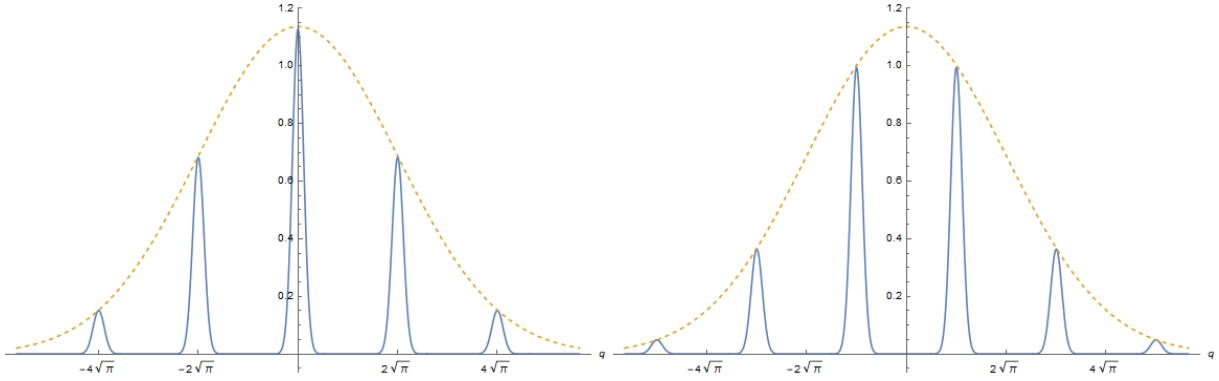


Figure 2.2: Blue lines represent the absolute value of the wave functions $|\Psi(q)|^2$ of approximate code states in the \hat{q} quadrature with $\Delta = 0.2$. Left figure is for the approximate state $|\tilde{0}\rangle$. Right one is for the approximate state $|\tilde{1}\rangle$. The dashed orange line is the Gaussian envelope.

~~The state $|\tilde{0}\rangle$ is defined by the condition $\langle \tilde{0} | \hat{q} | \tilde{0} \rangle = 0$ and $\langle \tilde{0} | \hat{p} | \tilde{0} \rangle = 0$. The state $|\tilde{1}\rangle$ is defined by the condition $\langle \tilde{1} | \hat{q} | \tilde{1} \rangle = \sqrt{\pi}$ and $\langle \tilde{1} | \hat{p} | \tilde{1} \rangle = 0$.~~

2.2 Finitely Squeezed States

~~In this section, we consider the finitely squeezed states $|\tilde{0}\rangle$ and $|\tilde{1}\rangle$ in the \hat{q} quadrature. The state $|\tilde{0}\rangle$ is defined by the condition $\langle \tilde{0} | \hat{q} | \tilde{0} \rangle = 0$ and $\langle \tilde{0} | \hat{p} | \tilde{0} \rangle = 0$. The state $|\tilde{1}\rangle$ is defined by the condition $\langle \tilde{1} | \hat{q} | \tilde{1} \rangle = \sqrt{\pi}$ and $\langle \tilde{1} | \hat{p} | \tilde{1} \rangle = 0$.~~

~~The state $|\tilde{0}\rangle$ is defined by the condition $\langle \tilde{0} | \hat{q} | \tilde{0} \rangle = 0$ and $\langle \tilde{0} | \hat{p} | \tilde{0} \rangle = 0$. The state $|\tilde{1}\rangle$ is defined by the condition $\langle \tilde{1} | \hat{q} | \tilde{1} \rangle = \sqrt{\pi}$ and $\langle \tilde{1} | \hat{p} | \tilde{1} \rangle = 0$.~~

$$\begin{aligned}
 |\tilde{0}\rangle &\propto \sum_{s=-\infty}^{\infty} \int_{-\infty}^{\infty} e^{-\frac{\Delta^2}{2}(2s)^2\pi} e^{-\frac{1}{2\Delta^2}(q-2s\sqrt{\pi})^2} |q\rangle dq, \\
 |\tilde{1}\rangle &\propto \sum_{s=-\infty}^{\infty} \int_{-\infty}^{\infty} e^{-\frac{\Delta^2}{2}(2s+1)^2\pi} e^{-\frac{1}{2\Delta^2}(q-(2s+1)\sqrt{\pi})^2} |q\rangle dq.
 \end{aligned} \tag{2.10}$$

~~The state $|\tilde{0}\rangle$ is defined by the condition $\langle \tilde{0} | \hat{q} | \tilde{0} \rangle = 0$ and $\langle \tilde{0} | \hat{p} | \tilde{0} \rangle = 0$. The state $|\tilde{1}\rangle$ is defined by the condition $\langle \tilde{1} | \hat{q} | \tilde{1} \rangle = \sqrt{\pi}$ and $\langle \tilde{1} | \hat{p} | \tilde{1} \rangle = 0$.~~

is

$$\begin{aligned}
 |\tilde{+}\rangle &\propto \sum_{s=-\infty}^{\infty} \int_{-\infty}^{\infty} e^{-\frac{\Delta^2}{2}(2s)^2\pi} e^{-\frac{1}{2\Delta^2}(p-2s\sqrt{\pi})^2} |p\rangle dp, \\
 |\tilde{-}\rangle &\propto \sum_{s=-\infty}^{\infty} \int_{-\infty}^{\infty} e^{-\frac{\Delta^2}{2}(2s+1)^2\pi} e^{-\frac{1}{2\Delta^2}(p-(2s+1)\sqrt{\pi})^2} |p\rangle dp.
 \end{aligned}
 \tag{2.11}$$

Using (2.4) and

$$a^{-1/2} \sum_{s=-\infty}^{\infty} e^{-\pi s^2/a} e^{2i\pi tb} = \sum_{m=-\infty}^{\infty} e^{-\pi a(m-b)^2}$$

we find

$$|\tilde{0}\rangle$$

$$\begin{aligned}
 |\tilde{0}\rangle &= \sum_{s=-\infty}^{\infty} \int_{-\infty}^{\infty} e^{-\frac{\Delta^2}{2}(2s)^2\pi} e^{-\frac{1}{2\Delta^2}(q-2s\sqrt{\pi})^2} |q\rangle dq \\
 &= \sum_{s=-\infty}^{\infty} \int_{-\infty}^{\infty} e^{-\frac{\Delta^2}{2}(2s)^2\pi} e^{-\frac{1}{2\Delta^2}(q-2s\sqrt{\pi})^2} dq \int \frac{dp}{\sqrt{2\pi}} e^{ipq} |p\rangle \\
 &= \frac{\Delta}{\sqrt{2}} e^{-\frac{p^2\Delta^2}{2}} \cdot \underbrace{\int_{-\infty}^{\infty} e^{-\frac{1}{2\Delta^2}(q-2s\Delta^2\sqrt{\pi}-i\Delta^2p)^2} dq}_{\text{Gaussian Integral}} \cdot \underbrace{\frac{\sqrt{2}}{\Delta} \sum_{s=-\infty}^{\infty} e^{-\frac{2\pi s^2}{\Delta^2}} e^{2i\pi\Delta^2\frac{p}{\sqrt{\pi}}}}_{\text{Poisson Summation}} \\
 &\propto \sum_{s=-\infty}^{\infty} \int_{-\infty}^{\infty} e^{-\frac{\Delta^2}{2}s^2\pi} e^{-\frac{1}{2\Delta^2}(p-s\sqrt{\pi})^2} |p\rangle dp
 \end{aligned}$$

with

$$p \approx s\sqrt{\pi}$$

to

$$|\tilde{\Psi}\rangle,$$

$$|\bar{\Psi}\rangle$$

we

$$|\tilde{\Psi}\rangle \propto \int_{-\infty}^{\infty} \int_{-\infty}^{\infty} e^{-\frac{1}{2}\left(\frac{u^2}{\Delta^2}\right)} e^{-iu\hat{p}+iv\hat{q}} |\bar{\Psi}\rangle du dv,
 \tag{2.12}$$

and (2.12), we

$$|\tilde{0}\rangle \text{ and } |\tilde{1}\rangle$$

are

discussed in Sec. 2.1.2, and

are

discussed in

Sec. 3.3.1.

Using

we find

that

2.3 Internal Shift Errors due to Finite Squeezing

Using

we find

that

we find

that

we find

2.3.1 Shifted Code States in Two Quadratures

Following the definition of the shifted code states in two quadratures, we have

$$|u, v\rangle = \frac{1}{\sqrt[4]{\pi}} e^{-iv\hat{q}} e^{-iu\hat{p}} |\bar{0}\rangle, \quad (2.13)$$

where $|\bar{0}\rangle$ is the ground state of the harmonic oscillator with frequency $\omega = 2$ and mass $m = 1$. The ground state is given by

$$u \in [-\sqrt{\pi}, \sqrt{\pi}], \quad v \in [-\sqrt{\pi}/2, \sqrt{\pi}/2].$$

Using the definition of the shifted code states, we have

$$\begin{aligned} \langle u, v | u', v' \rangle &= \frac{1}{\sqrt{\pi}} \sum_{s, s'} e^{i(v(2s\sqrt{\pi}+u) - v'(2s'\sqrt{\pi}+u'))} \underbrace{\langle 2s\sqrt{\pi} + u | 2s'\sqrt{\pi} + u' \rangle}_{\delta_{s, s'} \delta(u-u')} \\ &= \frac{1}{\sqrt{\pi}} e^{iu(v-v')} \sum_s e^{is2\sqrt{\pi}(v-v')} \delta(u-u') \\ &= \delta(v-v') \delta(u-u'), \end{aligned}$$

where $\delta(x) = \frac{1}{2\pi} \sum_s e^{isx}$ and $\delta(ax) = \frac{1}{|a|} \delta(x)$. Using the definition of the shifted code states, we have

$$|\tilde{\phi}\rangle = \frac{1}{\sqrt{2}} (|\bar{0}\rangle + |\bar{1}\rangle),$$

where

$|\bar{0}\rangle$ and $|\bar{1}\rangle$ are the ground and first excited states of the harmonic oscillator with frequency $\omega = 2$ and mass $m = 1$.

Using the definition of the shifted code states, we have

$|\bar{0}\rangle = \frac{1}{\sqrt{2}} (|\bar{0}\rangle + |\bar{1}\rangle)$

and $|\bar{1}\rangle = \frac{1}{\sqrt{2}} (|\bar{0}\rangle - |\bar{1}\rangle)$.

$$|u, v_1\rangle = |u, v_2 \pm \sqrt{\pi}\rangle_q = \frac{1}{\sqrt[4]{\pi}} e^{-iv_2\hat{q}} e^{\pm i\sqrt{\pi}\hat{q}} e^{-iu\hat{p}} |\bar{0}\rangle = |u, v_2\rangle,$$

where

$|\bar{0}\rangle$ and $|\bar{1}\rangle$ are the ground and first excited states of the harmonic oscillator with frequency $\omega = 2$ and mass $m = 1$.

Using the definition of the shifted code states, we have

$|\bar{0}\rangle = \frac{1}{\sqrt{2}} (|\bar{0}\rangle + |\bar{1}\rangle)$

and $|\bar{1}\rangle = \frac{1}{\sqrt{2}} (|\bar{0}\rangle - |\bar{1}\rangle)$.

$$|u, v\rangle = \frac{1}{\sqrt[4]{\pi}} e^{-iv\hat{q}} e^{-iu\hat{p}} |\bar{0}\rangle, \quad p \in [-\sqrt{\pi}/2, \sqrt{\pi}/2]$$

$$|u, v\rangle_q = |u, v\rangle. \quad (2.14)$$

Using the definition of the shifted code states, we have

$|\bar{0}\rangle = \frac{1}{\sqrt{2}} (|\bar{0}\rangle + |\bar{1}\rangle)$

and $|\bar{1}\rangle = \frac{1}{\sqrt{2}} (|\bar{0}\rangle - |\bar{1}\rangle)$.

$$\begin{aligned} |u, v\rangle_p &= \frac{1}{\sqrt[4]{\pi}} e^{-iv\hat{q}} e^{-iu\hat{p}} |\bar{+}\rangle, \\ u &\in [-\sqrt{\pi}/2, \sqrt{\pi}/2], \\ v &\in [-\sqrt{\pi}, \sqrt{\pi}]. \end{aligned} \quad (2.15)$$

The state $|u, v\rangle_p$ is defined as

$$|u, v\rangle_p = \frac{1}{\sqrt{2\pi}} \int_{-\sqrt{\pi}}^{\sqrt{\pi}} du \int_{-\frac{\sqrt{\pi}}{2}}^{\frac{\sqrt{\pi}}{2}} dv \langle u, v | \Phi \rangle \cdot |u, v\rangle,$$
 where $|u, v\rangle_q$ is the state in the q basis.

2.3.2 Approximate Internal Shift Error Probability Distributions

The state $|\Phi\rangle$ is

$$|\Phi\rangle = \int_{-\sqrt{\pi}}^{\sqrt{\pi}} du \int_{-\frac{\sqrt{\pi}}{2}}^{\frac{\sqrt{\pi}}{2}} dv \langle u, v | \Phi \rangle \cdot |u, v\rangle, \quad (2.16)$$

The state $|u, v\rangle = |u, v\rangle_q$ is defined as

$$|u, v\rangle_p = \frac{1}{\sqrt{2\pi}} \int_{-\sqrt{\pi}}^{\sqrt{\pi}} du \int_{-\frac{\sqrt{\pi}}{2}}^{\frac{\sqrt{\pi}}{2}} dv \langle u, v | \Phi \rangle \cdot |u, v\rangle,$$
 where $|u, v\rangle_q$ is the state in the q basis.

$$P(u, v) = P(u, v | \Phi) = |\langle u, v | \Phi \rangle|^2.$$

The state $|\Phi\rangle$ is

$$\begin{aligned}
 P(u, v) &= |\langle u, v | \tilde{0} \rangle|^2 \\
 &= \frac{2}{\pi} \sum_{t, t'} \sum_{s, s'} e^{iv(2t-2t')\sqrt{\pi}} e^{-2\pi\Delta^2(s^2+s'^2)} e^{-(u+(2t'-2s')\sqrt{\pi})^2/(2\Delta^2)} e^{-(u+(2t-2s)\sqrt{\pi})^2/(2\Delta^2)} \\
 &= \frac{2}{\pi} \sum_{t, t'} \sum_{s, s'} e^{iv(2t-2t')\sqrt{\pi}} e^{-2\pi\Delta^2(s^2+s'^2)} e^{-\frac{u^2}{\Delta^2}} e^{-\frac{2(t+t'-s-s')\sqrt{\pi}}{\Delta^2}} e^{-\frac{2((t-s)^2+(t'-s')^2)\pi}{\Delta^2}},
 \end{aligned}$$

For $e^{-\frac{2\pi}{\Delta^2}} \ll 1$, i.e. $\Delta \ll \sqrt{2\pi} \approx 2.5$, the state $|\Phi\rangle$ is

$$|\Phi\rangle = \frac{1}{\sqrt{2\pi}} \int_{-\sqrt{\pi}}^{\sqrt{\pi}} du \int_{-\frac{\sqrt{\pi}}{2}}^{\frac{\sqrt{\pi}}{2}} dv \langle u, v | \Phi \rangle \cdot |u, v\rangle,$$
 where $t = s$ and $t' = s'$.

$$\begin{aligned}
 P(u, v) &\approx \frac{2}{\pi} \sum_{s, s'} e^{iv(2s-2s')\sqrt{\pi}} e^{-2\pi\Delta^2(s^2+s'^2)} e^{-\frac{u^2}{\Delta^2}} \\
 &= \underbrace{\left[\frac{2\Delta}{\sqrt{\pi}} \sum_{s, s'} e^{iv(2s-2s')\sqrt{\pi}} e^{-2\pi\Delta^2(s^2+s'^2)} \right]}_{\text{only depends on } v} \underbrace{\left[\frac{1}{\frac{\Delta}{\sqrt{2}} \cdot \sqrt{2\pi}} e^{-\frac{u^2}{2\left(\frac{\Delta}{\sqrt{2}}\right)^2}} \right]}_{\text{Gaussian only depends on } u} \quad (2.17)
 \end{aligned}$$

$P(u, v)$ is the probability density function of u and v . The joint probability density function $P(u, v)$ is given by

$$\begin{aligned}
 P(u) &= \int_{-\frac{\sqrt{\pi}}{2}}^{\frac{\sqrt{\pi}}{2}} dv P(u, v) \\
 &= \sum_{s, s'} \underbrace{\int_{-\frac{\sqrt{\pi}}{2}}^{\frac{\sqrt{\pi}}{2}} dv e^{iv(2s-2s')\sqrt{\pi}}}_{\sqrt{\pi}\delta_{s, s'}} \left[\frac{2\Delta}{\sqrt{\pi}} e^{-2\pi\Delta^2(s^2+s'^2)} \right] \underbrace{\frac{1}{\frac{\Delta}{\sqrt{2}} \cdot \sqrt{2\pi}} e^{-\frac{u^2}{2\left(\frac{\Delta}{\sqrt{2}}\right)^2}}}_{\text{Gaussian}} \\
 &= \underbrace{\left[2\Delta \sum_s e^{-4\pi\Delta^2 s^2} \right]}_{\text{a constant}} \underbrace{\frac{1}{\frac{\Delta}{\sqrt{2}} \cdot \sqrt{2\pi}} e^{-\frac{u^2}{2\left(\frac{\Delta}{\sqrt{2}}\right)^2}}}_{\text{Gaussian}}.
 \end{aligned}$$

For $\Delta \lesssim 0.4$, $\sum_s e^{-4\pi\Delta^2 s^2} \rightarrow 1$.

$$u \sim \mathcal{N}\left(0, \frac{\Delta}{\sqrt{2}}\right). \quad (2.18)$$

The state $|\Phi\rangle = \alpha|\tilde{0}\rangle + \beta|\tilde{1}\rangle$, $|\langle u, v|\tilde{0}\rangle|^2$ and $|\langle u, v|\tilde{1}\rangle|^2$ are given by

$$|\Phi\rangle = \alpha|\tilde{+}\rangle + \beta|\tilde{-}\rangle, \quad |u, v\rangle_p$$

u, v are the quadratures.

2.4 Gaussian Shift Error Channel

The state $|\tilde{\psi}\rangle$ is given by

$$|\tilde{\psi}\rangle = \int du dv \sqrt{P_u P_v} e^{-iu\hat{p} + iv\hat{q}} |\psi\rangle$$

where P_u, P_v are the probability density functions of u, v .

\mathcal{E} :

$$\rho \rightarrow \mathcal{E}(\rho) = \int d\alpha d\alpha' \mathcal{P}(\alpha, \alpha') D(\alpha) \rho D^\dagger(\alpha') \quad (2.19)$$

where $\alpha = u - iv$ and $\mathcal{P}(\alpha, \alpha') = \sqrt{P_u P_v P_u' P_v'}$. The displacement operator $D(\alpha)$ is

$$D(\alpha) = e^{i\alpha\hat{a}^\dagger - \alpha^*\hat{a}},$$

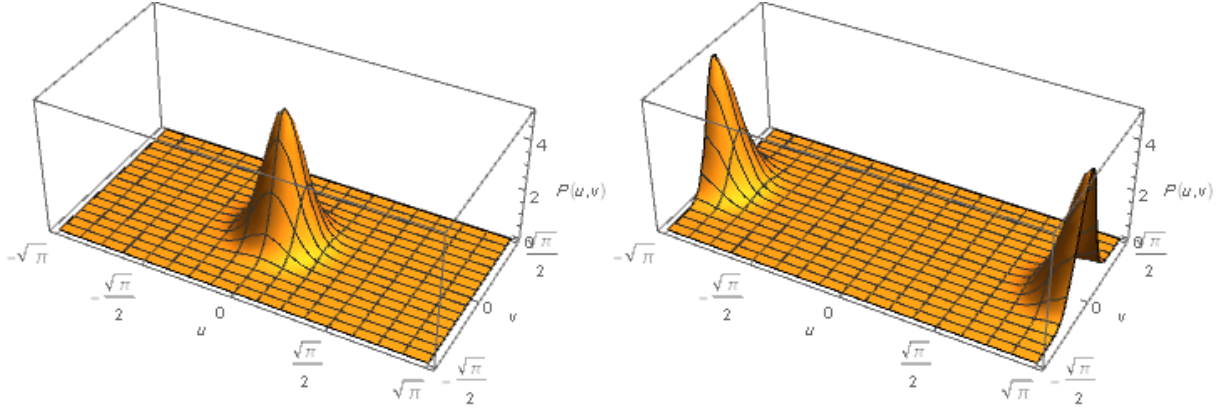


Figure 2.3: Probability density of approximate code states' shift errors with the squeezing parameter $\Delta = 0.25$, using the shifted code states in the \hat{q} quadrature $|u, v\rangle_q$. Where u, v are the shift errors in the \hat{q} quadrature and the \hat{p} quadrature respectively. Left one is for approximate state $|\hat{0}\rangle$. The right one is for approximate state $|\hat{1}\rangle$. The probability distribution is periodic with respect to $u \in [-\sqrt{\pi}, \sqrt{\pi}]$ and $v \in [-\sqrt{\pi}/2, \sqrt{\pi}/2]$, so only one peak in that range is shown here.

is given by the displacement operator $D(\alpha) = \exp(-iu\hat{p} + iv\hat{q})$. Using (2.4.1), we can write the probability density as

$$\rho \rightarrow \mathcal{E}(\rho) = \int du dv P_u P_v D(u, v) \rho D^\dagger(u, v). \quad (2.20)$$

where $P_u = P_\sigma(u)$ and $P_v = P_\sigma(v)$.

The displacement operator $D(u, v)$ acts on the quadratures q and p as

$$q \rightarrow q + u \quad p \rightarrow p + v$$

2.4.1 Generalized Pauli Twirling Approximation

Consider a state ρ and a set of Pauli matrices $\mathcal{P} = \{I, X, Y, Z\}$.

$$\rho \rightarrow \mathcal{E}'(\rho) = \sum_{n,m=1}^4 \chi_{m,n} B_m \rho B_n^\dagger \quad (2.21)$$

where χ is a matrix and B_m are Pauli matrices. The Pauli matrices are $\mathcal{P} = \{I, X, Y, Z\}$. The Pauli matrices are B_k .

$$\begin{aligned} \rho \rightarrow \bar{\mathcal{E}}'(\rho) &= \frac{1}{K} \sum_{k=1}^K \mathbb{B}_k^\dagger \mathcal{E}(\mathbb{B}_k \rho \mathbb{B}_k^\dagger) \mathbb{B}_k \\ &= \sum_{n=1}^4 P_n B_n \rho B_n^\dagger \end{aligned} \quad (2.22)$$

using (2.21) and

P_n is

the integral of \mathcal{E} in (2.19) over $D(\beta)$ with respect to β .

$$\bar{\mathcal{E}}(\rho) = \frac{1}{\mathcal{N}} \int d\beta D^\dagger(\beta) \mathcal{E}(D(\beta)\rho D^\dagger(\beta)) D(\beta) \quad (2.23)$$

in \mathcal{N} is

$$\frac{1}{\mathcal{N}} \int d\beta = \int d\beta$$

in (2.20). In the limit

$\beta \rightarrow \infty$,

β is

is

$$\frac{1}{\gamma\pi} \int d\beta e^{-\frac{|\beta|^2}{\gamma}} \quad (2.24)$$

is

$$\bar{\mathcal{E}}(\rho) = \frac{1}{\gamma\pi} \int d\beta e^{-\frac{|\beta|^2}{\gamma}} D^\dagger(\beta) \mathcal{E}(D(\beta)\rho D^\dagger(\beta)) D(\beta) \quad (2.25)$$

is

$$D(\alpha)D(\beta) = e^{(\alpha\beta^* - \beta\alpha^*)/2} D(\alpha + \beta),$$

$$\bar{\mathcal{E}}(\rho) = \int d\alpha \int d\alpha' P(\alpha, \alpha') D(\alpha)\rho D^\dagger(\alpha') \cdot \underbrace{\frac{1}{\gamma\pi} \int d\beta e^{-\frac{|\beta|^2}{\gamma}} e^{[(\alpha\beta^* - \beta\alpha^*) - (\alpha'\beta^* - \beta\alpha'^*)]}}_{e^{-\gamma|\alpha - \alpha'|^2}} \quad (2.26)$$

$$= \int d\alpha D(\alpha)\rho \int d\alpha' P(\alpha, \alpha') D^\dagger(\alpha') e^{-\gamma|\alpha - \alpha'|}, \quad (2.27)$$

is

γ is

$$\gamma \gg \frac{1}{|\alpha - \alpha'|^2}, \quad (2.28)$$

is

$\alpha \neq \alpha'$ is

is

$$\bar{\mathcal{E}}(\rho) \propto \int d\alpha P(\alpha) D(\alpha)\rho D^\dagger(\alpha), \quad (2.29)$$

is $P(\alpha) = P(\alpha, \alpha)$ is

in (2.20). In

$\gamma \rightarrow \infty$, (2.24) is

is

in (2.23).

2.4.2 Comparing Two Kinds of Shift Errors

is

is

is

$$|\tilde{\psi}\rangle \quad \sigma:$$

$$|\tilde{\psi}\rangle = \int du dv \sqrt{P_\sigma(u)P_\sigma(v)} \cdot e^{-iu\hat{p}} e^{iv\hat{q}} |\psi\rangle, \quad (2.30)$$

In $|\tilde{\psi}\rangle$ ist $\tilde{\rho}$ die
 Dichte
 in $|\psi\rangle$ ist
 die Dichte

$|\psi\rangle$ ist
 σ .
 ρ :

$$\tilde{\rho} = \int du dv P_\sigma(u) P_\sigma(v) \cdot e^{-iu\hat{p}} e^{iv\hat{q}} |\psi\rangle \langle\psi| e^{+iu\hat{p}} e^{-iv\hat{q}}. \quad (2.31)$$

Die Dichte $\tilde{\rho}$ ist
 die Dichte
 in $|\psi_{out}\rangle$ ist

u, v sind

u_0, v_0 :

$$|\psi_{out}\rangle = e^{-iu_0\hat{p}} e^{iv_0\hat{q}} |\psi\rangle, \quad (2.32)$$

Die Dichte $\tilde{\rho}$ ist
 die Dichte
 in $|\psi_{out}\rangle$ ist

$$P(u_0, v_0) = P_\sigma(u_0) P_\sigma(v_0).$$

u_0, v_0 .

Die Dichte $\tilde{\rho}$ ist
 die Dichte
 in $|\psi_{out}\rangle$ ist

Quantum Computation with GKP Code States

3.1 Clifford Gates of GKP code states
 3.2
 3.3
 3.4

3.1 Clifford Gates of GKP code states

The Clifford gates are defined as follows:

\mathbb{C}	$X_1 \rightarrow X_1 X_2$	$Z_1 \rightarrow Z_1$
	$X_2 \rightarrow X_2$	$Z_2 \rightarrow Z_1 Z_2$
\mathbb{H}	$H : X \rightarrow Z$	$Z \rightarrow X$
\mathbb{R}	$S : X \rightarrow iXZ$	$Z \rightarrow Z$

The Clifford gates are defined as follows:

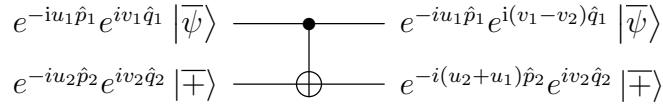


Figure 3.1: Circuit of the CNOT gate, where $|\bar{\psi}\rangle$ represents an arbitrary ideal GKP code state. The logical CNOT gate moves the shift error u_1 of $|\bar{\psi}\rangle$ to $|+\rangle$, and moves the shift error v_2 in the opposite direction.

3.1.1 Action on the GKP Code States

Consider the GKP code

$$|\psi\rangle = \int_{\mathbb{R}^2} d^2\alpha \hat{X}^{\alpha_1} \hat{Z}^{\alpha_2} |\psi_0\rangle$$

is defined

$$q_i \hat{d}^\dagger - p_i \hat{a}$$

$$U_{\alpha\beta} = \exp \left[i\sqrt{2\pi} \left(\sum_{i=1}^N \alpha_i \hat{p}_i + \beta_i \hat{q}_i \right) \right],$$

where α_i and β_i are real numbers.

is defined

$$\bar{X} = e^{i\sqrt{\pi}\hat{p}}, \quad \bar{Z} = e^{i\sqrt{\pi}\hat{q}}.$$

Consider the GKP code

is defined

$$|\psi\rangle = \int_{\mathbb{R}^2} d^2\alpha \hat{X}^{\alpha_1} \hat{Z}^{\alpha_2} |\psi_0\rangle$$

is defined

is defined

$$\begin{aligned} \mathbb{N} & \hat{d}^\dagger & q_1 & \rightarrow \hat{q}_1 & \hat{p}_1 & \rightarrow \hat{p}_1 + \hat{p}_2 \\ & & \hat{q}_2 & \rightarrow \hat{q}_2 - \hat{q}_1 & \hat{p}_2 & \rightarrow \hat{p}_2 \\ \mathbb{H} & H & \hat{q} & \rightarrow \hat{p} & \hat{p} & \rightarrow -\hat{q} \\ \mathbb{R} & S & \hat{q} & \rightarrow \hat{q} & \hat{p} & \rightarrow \hat{p} - \hat{q} \end{aligned}$$

Consider the GKP code

is defined

is defined

3.1.2 Error Propagation

Consider the GKP code

is defined

$$|\psi_{in}\rangle \propto e^{i(u_1 \hat{p}_1 + u_2 \hat{p}_2)} e^{i(v_1 \hat{q}_1 + v_2 \hat{q}_2)} |\bar{\psi}_1, \bar{\psi}_2\rangle.$$

Equation (3.1) is (proof):

$$\begin{aligned}
 C_x : |\psi_{in}\rangle &\rightarrow C_x e^{i(u_1 \hat{p}_1 + u_2 \hat{p}_2)} e^{i(v_1 \hat{q}_1 + v_2 \hat{q}_2)} C_x^\dagger \cdot C_x |\bar{\psi}_1, \bar{\psi}_2\rangle \\
 &\propto e^{i[u_1(\hat{p}_1 + \hat{p}_2) + u_2 \hat{p}_2]} e^{i[v_1 \hat{q}_1 + v_2(\hat{q}_2 - \hat{q}_1)]} \cdot C_x |\bar{\psi}_1, \bar{\psi}_2\rangle \\
 &\propto e^{i[u_1 \hat{p}_1 + (v_1 - v_2) \hat{q}_1]} e^{i[(u_2 + u_1) \hat{p}_2 + v_2 \hat{q}_2]} \cdot C_x |\bar{\psi}_1\rangle |\bar{\psi}_2\rangle.
 \end{aligned}$$

Is this the same as the Hadamard gate? The Hadamard gate is defined as $H = \frac{1}{\sqrt{2}} \begin{pmatrix} 1 & 1 \\ 1 & -1 \end{pmatrix}$. The Hadamard gate is a unitary operation that maps the computational basis states $|0\rangle$ and $|1\rangle$ to the Hadamard basis states $|+\rangle$ and $|-\rangle$. The Hadamard gate is a special case of the C_x gate with $u_1 = 1, u_2 = 1, v_1 = 1, v_2 = 1$.

3.2 Universal Quantum Computation

Equation (3.1) is (proof):

$$\begin{aligned}
 &\pi/8 \text{ gate} \\
 &\pi/8 \text{ gate} \\
 &\pi/8 \text{ gate} \\
 &\text{et al. } \S
 \end{aligned}$$

3.2.1 The $\pi/8$ Gate using Hadamard Eigenstate

Equation (3.1) is (proof):

$$|\Psi_{H=1}\rangle = \frac{1}{\sqrt{2}} (|0\rangle + |1\rangle).$$

Equation (3.1) is (proof):

$$H \cdot S^{-1} = \frac{1}{\sqrt{2}} \begin{pmatrix} 1 & 1 \\ 1 & -1 \end{pmatrix} \cdot \begin{pmatrix} 1 & 0 \\ 0 & -i \end{pmatrix} = \frac{1}{\sqrt{2}} \begin{pmatrix} 1 & -i \\ 1 & i \end{pmatrix}.$$

Equation (3.1) is (proof):

$$|\Psi_{\pi/8}\rangle = \frac{1}{\sqrt{2}} (e^{-i\pi/8} |0\rangle + e^{i\pi/8} |1\rangle).$$

Equation (3.1) is (proof):

$$T = \begin{pmatrix} e^{-i\pi/8} & 0 \\ 0 & e^{i\pi/8} \end{pmatrix}.$$

Equation (3.1) is (proof):

$$|\Psi_{\pi/8}\rangle = T |+\rangle$$

$$|\Psi_{\pi/8}\rangle = T |+\rangle$$

Equation (3.1) is (proof):

$$|\phi\rangle \text{ [3] } T \text{ gate } \pi/8$$

Equation (3.1) is (proof):

Equation (3.1) is (proof):

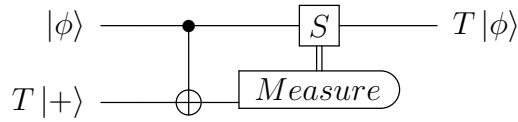


Figure 3.2: Circuit for gate teleportation. The data qubit is in an arbitrary state $|\phi\rangle$. The ancilla qubit is in state $|\Phi_{\pi/8}\rangle = T|+\rangle$. Measure the ancilla in the basis $|0\rangle, |1\rangle$, and apply a conditional phase gate S on the data qubit. The output qubit is in state $T|\phi\rangle$ up to some phase factors.

3.2.2 Photon Number Modulo Four

Introduction

\mathcal{H} is

$$\mathcal{H} = \hbar\omega\left(\hat{a}^\dagger\hat{a} + \frac{1}{2}\right), \quad (3.1)$$

where \hbar is Planck's constant, ω is the angular frequency, and t is time.

ω is the

$$U(t) = e^{-\frac{i}{\hbar}\mathcal{H}t} = e^{-i\omega t\hat{a}^\dagger\hat{a}}. \quad (3.2)$$

Effect of \hat{a}

q and p are

$$\begin{aligned} \hat{q} &\rightarrow U^\dagger(t)\hat{q}U(t) \propto \hat{a}e^{-i\omega t} + \hat{a}^\dagger e^{i\omega t}, \\ \hat{p} &\rightarrow U^\dagger(t)\hat{p}U(t) \propto \hat{a}e^{-i\omega t} - \hat{a}^\dagger e^{i\omega t}. \end{aligned} \quad (3.3)$$

is given

$$t = \frac{\pi}{2\omega}, \quad (3.3) \text{ is valid}$$

that $H^\dagger\hat{q}H \rightarrow \hat{p}$ and $H^\dagger\hat{p}H \rightarrow -\hat{q}$, see 3.1. This

applies

$$H : \mathbb{R}^2 \left(i\frac{\pi}{2}\hat{a}^\dagger\hat{a} \right),$$

which is a rotation by $\pi/2$ in phase space.

For $n=0$ or

$n=1$, the

transformations $q \rightarrow -\hat{q}, \hat{p} \rightarrow -\hat{p}$, which is a

rotation by π in phase space.

For $t = \frac{\pi}{\omega}$, see (3.3). This is

the same as

$$U(t = \pi/\omega):$$

$$U(t = \pi/\omega) |n\rangle = e^{in\pi} |n\rangle = |n\rangle.$$

For

n is an integer

the

3.2.3 Preparing a Hadamard Eigenstate

Introduction

et al. [1]

Consider the

Hamiltonian

$$\mathcal{H}' = \hbar\omega'\hat{a}^\dagger\hat{a}\sigma_z,$$

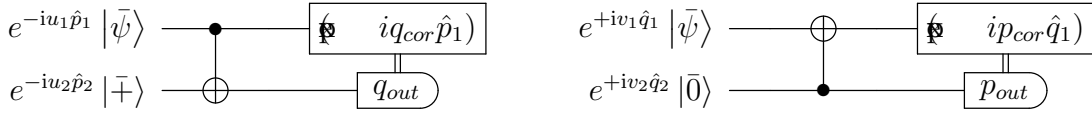


Figure 3.3: Circuits of the Steane error correction scheme. The left circuit corrects shift errors in the \hat{q} quadrature and right one in the \hat{p} quadrature. The logical CNOT moves the shift errors as discussed in Sec. 3.1.2. We have incoming shift errors $u_1, v_1 \in [-\sqrt{\pi}/2, \sqrt{\pi}/2]$. And ancilla qubits $|\bar{+}\rangle, |0\rangle$ have shift error $u_2, v_2 \in [-\sqrt{\pi}/2, \sqrt{\pi}/2]$. After the CNOT gate, we measure the ancillas in q, p quadratures respectively and get the homodyne measurement outcomes $q_{out} = u_1 + u_2 + n_1\sqrt{\pi}$ and $p_{out} = -v_1 + v_2 + n_2\sqrt{\pi}$ with n_1, n_2 arbitrary integers. Then we calculate $q_{cor} = q_{out} \bmod \sqrt{\pi} \in [-\sqrt{\pi}/2, \sqrt{\pi}/2]$ and apply the correction operators, which is the same for p_{cor} .

$$\sigma_z |0\rangle_a = -|0\rangle_a \quad \sigma_z |1\rangle_a = |1\rangle_a$$

$$t = \frac{\pi}{4\omega'}, \quad t = \pi/(4\omega')$$

$$U(t = \frac{\pi}{4\omega'}) = -i(\pi/4)\hat{a}^\dagger\hat{a}\sigma_z.$$

$$\frac{1}{\sqrt{2}}(|0\rangle_a + |1\rangle_a) |n\rangle$$

$$\begin{aligned} \frac{1}{\sqrt{2}}(|0\rangle_a + |1\rangle_a) |n\rangle &\rightarrow U(t = \frac{\pi}{4\omega'}) \cdot \frac{1}{\sqrt{2}}(|0\rangle_a + |1\rangle_a) |n\rangle \\ &= \frac{1}{\sqrt{2}}(e^{in\pi/4} |0\rangle_a + e^{-in\pi/4} |1\rangle_a) |n\rangle \\ &= \frac{1}{\sqrt{2}}e^{in\pi/4} \cdot (|0\rangle_a + e^{-in\pi/2} |1\rangle_a) \cdot |n\rangle. \end{aligned}$$

$$\frac{1}{\sqrt{2}}(|0\rangle_a + |1\rangle_a), \quad \frac{1}{\sqrt{2}}(|0\rangle_a - |1\rangle_a)$$

$$|0\rangle_a \pm |1\rangle_a)/\sqrt{2}, \quad n = 0$$

3.3 Steane Error Correction Scheme

Figure 3.3. The left circuit corrects shift errors in the \hat{q} quadrature and right one in the \hat{p} quadrature. The logical CNOT moves the shift errors as discussed in Sec. 3.1.2. We have incoming shift errors $u_1, v_1 \in [-\sqrt{\pi}/2, \sqrt{\pi}/2]$. And ancilla qubits $|\bar{+}\rangle, |0\rangle$ have shift error $u_2, v_2 \in [-\sqrt{\pi}/2, \sqrt{\pi}/2]$. After the CNOT gate, we measure the ancillas in q, p quadratures respectively and get the homodyne measurement outcomes $q_{out} = u_1 + u_2 + n_1\sqrt{\pi}$ and $p_{out} = -v_1 + v_2 + n_2\sqrt{\pi}$ with n_1, n_2 arbitrary integers. Then we calculate $q_{cor} = q_{out} \bmod \sqrt{\pi} \in [-\sqrt{\pi}/2, \sqrt{\pi}/2]$ and apply the correction operators, which is the same for p_{cor} .

$$e^{-iu_1\hat{p}_1} e^{-iu_2\hat{p}_2} |\bar{\psi}\rangle |\bar{+}\rangle. \quad (3.4)$$

3.3. The

is a solution to the problem of quantum error correction. The code is defined by the stabilizer group

$$e^{-iu_1\hat{p}_1} e^{-iu_2\hat{p}_2} |\bar{\psi}\rangle_1 |\bar{\psi}\rangle_2 \rightarrow e^{-iu_1\hat{p}_1} e^{-i(u_1+u_2)\hat{p}_2} |\bar{\psi}\rangle_1 |\bar{\psi}\rangle_2, \quad (3.5)$$

is a solution to the problem of quantum error correction. The code is defined by the stabilizer group

$$\begin{aligned} &= \sum_{s,s' \in \mathbb{Z}} \alpha |q_1 = s\sqrt{\pi} + u\rangle |q_2 = (s+s')\sqrt{\pi} + u\rangle \\ &\quad + \beta |q_1 = (s+1)\sqrt{\pi} + u\rangle |q_2 = (s+1+s')\sqrt{\pi} + u\rangle \\ &= \sum_{n_0, n_1 \in \mathbb{Z}} \left(\alpha |q_1 = n_0\sqrt{\pi} + u_1\rangle + \beta |q_1 = (n_0+1)\sqrt{\pi} + u_1\rangle \right) |q_2 = n_1\sqrt{\pi} + u_1 + u_2\rangle, \end{aligned} \quad (3.6)$$

is a solution to the problem of quantum error correction. The code is defined by the stabilizer group

$$|\bar{\psi}\rangle = \alpha |\bar{0}\rangle + \beta |\bar{1}\rangle \quad |\alpha|^2 + |\beta|^2 = 1. \quad q_{out} = u_1 + u_2 + n_1\sqrt{\pi}, \quad n_1 \in \mathbb{Z}.$$

is a solution to the problem of quantum error correction. The code is defined by the stabilizer group

$$\begin{aligned} &\sum_{s \in \mathbb{Z}} \left(\alpha |q_1 = s\sqrt{\pi} - u_2 - n_1\sqrt{\pi}\rangle + \beta |q_1 = (s+1)\sqrt{\pi} - u_2 - n_1\sqrt{\pi}\rangle \right) \\ &= e^{in_1\sqrt{\pi}\hat{p}} e^{iu_2\hat{p}} |\bar{\psi}\rangle, \end{aligned}$$

is a solution to the problem of quantum error correction. The code is defined by the stabilizer group

$$\begin{aligned} &\sqrt{\pi} \text{ is a solution to the problem of quantum error correction. The code is defined by the stabilizer group} \\ &X \text{ is a solution to the problem of quantum error correction. The code is defined by the stabilizer group} \\ &|\bar{0}\rangle \text{ is a solution to the problem of quantum error correction. The code is defined by the stabilizer group} \end{aligned}$$

is a solution to the problem of quantum error correction. The code is defined by the stabilizer group

$$u_1 \rightarrow -u_2, \quad v_1 \rightarrow v_1 - v_2, \quad (3.7)$$

is a solution to the problem of quantum error correction. The code is defined by the stabilizer group

$$u_1 \rightarrow u_1 + u_2, \quad v_1 \rightarrow v_2, \quad (3.8)$$

is a solution to the problem of quantum error correction. The code is defined by the stabilizer group

$$|v_2 - v_1| < \frac{\sqrt{\pi}}{2}. \quad u, v \text{ is a solution to the problem of quantum error correction. The code is defined by the stabilizer group}$$

3.3.1 Steane Error Correction is Fault-Tolerant

is a solution to the problem of quantum error correction. The code is defined by the stabilizer group

$$\sqrt{\pi}/6 \text{ is a solution to the problem of quantum error correction. The code is defined by the stabilizer group}$$

Using the definition of the Hadamard gate, we can write the state as

$$\frac{1}{\sqrt{2}} \left(|0\rangle + |1\rangle \right) \otimes \frac{1}{\sqrt{2}} \left(|0\rangle + |1\rangle \right)$$

$$u_1, v_1 \rightarrow -u_2, v_1 - v_2,$$

$$|u_1 + u_2| < \sqrt{\pi}/2.$$

$$-u_2, v_1 - v_2 \rightarrow -u_2 + u_3, v_3,$$

$$|-v_1 + v_2 + v_3| < \sqrt{\pi}/2.$$

$$u_4, v_4,$$

$$-u_2 + u_3, v_3 \rightarrow -u_4, v_3 - v_4,$$

$$|-u_2 + u_3 + u_4| < \sqrt{\pi}/2.$$

$$-u_4, v_3 - v_4 \rightarrow -u_4 + u_5, v_5,$$

$$|-v_3 + v_4 + v_5| < \sqrt{\pi}/2.$$

The state is now

$$\frac{1}{\sqrt{2}} \left(|0\rangle + |1\rangle \right) \otimes \frac{1}{\sqrt{2}} \left(|0\rangle + |1\rangle \right)$$

3.3.2 Steane Error Correction with 1-Bit Teleportation

We start with a 7-qubit state

$$\frac{1}{\sqrt{2}} \left(|0\rangle + |1\rangle \right) \otimes \frac{1}{\sqrt{2}} \left(|0\rangle + |1\rangle \right)$$

$$\sum_{s,s' \in \mathbb{Z}} \left(\alpha |q_1 \oplus s\sqrt{\pi} + u_1 + u_2\rangle + \beta |q_1 \oplus (s+1)\sqrt{\pi} + u_1 + u_2\rangle \right) |q_2 \oplus s'\sqrt{\pi} + u_2\rangle$$

$$+ \sum_{s,s' \in \mathbb{Z}} \left(\alpha |q_1 \oplus (s+1)\sqrt{\pi} + u_1 + u_2\rangle + \beta |q_1 \oplus s\sqrt{\pi} + u_1 + u_2\rangle \right) |q_2 \oplus (s'+1)\sqrt{\pi} + u_2\rangle$$



Figure 3.4: Circuits for Steane error corrections via 1-bit teleportation. Left circuit corrects errors in the \hat{q} quadrature. After the CNOT gate we measure the data qubit in the \hat{q} quadrature with outcome $q_{out} = u_1 + u_2 + n\sqrt{\pi}, n \in \mathbb{Z}$. Based on q_{out} , we need to decide the state of data qubit after measurement, i.e. whether q_{out} is closer to an even multiple of $\sqrt{\pi}$ or closer to an odd multiple. If it's in $|0\rangle$, the ancilla will be left in state $|\bar{\psi}\rangle$ or with shift error u_2 and $v_1 + v_2$, otherwise there would be a logical error. The analysis for the left circuit which corrects errors in the \hat{p} quadrature is the same.

with

$$\sum_{s,s' \in \mathbb{Z}} \left(|q_1 \equiv s\sqrt{\pi} + u_1 + u_2\rangle (\alpha |q_2 \equiv s'\sqrt{\pi} + u_2\rangle + \beta |q_2 \equiv (s'+1)\sqrt{\pi} + u_2\rangle) \right. \\ \left. + |q_1 \equiv (s+1)\sqrt{\pi} + u_1 + u_2\rangle (\beta |q_2 \equiv s'\sqrt{\pi} + u_2\rangle + \alpha |q_2 \equiv (s'+1)\sqrt{\pi} + u_2\rangle) \right)$$

with

$$\sum_{s \in \mathbb{Z}} \left(|q_1 \equiv s\sqrt{\pi} + u_1 + u_2\rangle e^{-iu_2 \hat{p}_2} |\bar{\psi}\rangle + |q_1 \equiv (s+1)\sqrt{\pi} + u_1 + u_2\rangle e^{-iu_2 \hat{p}_2} \bar{X} |\bar{\psi}\rangle \right).$$

with $q_{out} = n\sqrt{\pi} + u_1 + u_2, n \in \mathbb{Z}$. If n is even, the data qubit is left in state $|\bar{\psi}\rangle$ or with shift error u_2 . If n is odd, the data qubit is left in state $\bar{X} |\bar{\psi}\rangle$ or with shift error $v_1 + v_2$.

with $|u_1 + u_2| \leq \sqrt{\pi}/2$.

3.4 Measurement-Based Quantum Computation with GKP Code

with $[2][1]$

with $F_{3.5}$

with $|+\rangle (|0\rangle^{\wedge} p \text{ or } |-\rangle)$

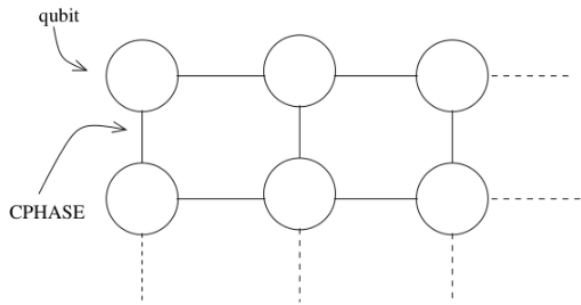


Figure 3.5: A two-dimensional cluster state. Blank nodes means qubits in state $|+\rangle$, the lines connecting qubits represent CPHASE gates.

is a [4]

$$K^{(a)} = \sigma_x^{(a)} \bigotimes_{b \in \text{neigh}(a)} \sigma_z^{(b)},$$

is a [4]

$$K^{(a)} = \sigma_x^{(a)} \bigotimes_{b \in \text{neigh}(a)} \sigma_z^{(b)}$$

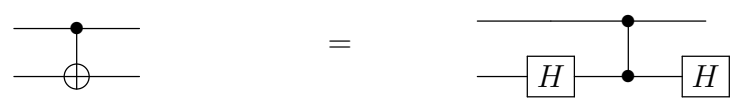
is a [4]

3.4.1 Steane Error Correction with Cluster States

is a [4]

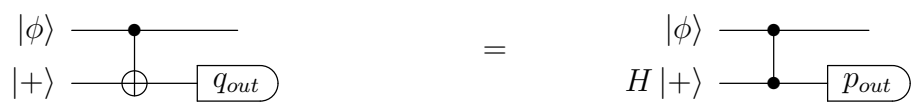
is a [4]

is a [4]



is a [4]

is a [4]



is a [4]

is a [4]

is a [4]

is a [4]

$$|0\rangle = H|+\rangle$$

is a [4]

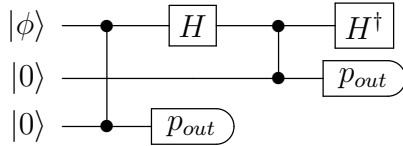


Figure 3.6: Circuit of quantum error correction consists of Steane error corrections in two quadratures. This circuit is equivalent to that in Fig. 3.3 up to correction operators. All three qubits are connected by CPHASE gates, and Hadamard gates is quite easy to be implemented through cluster state. It's quite obvious to notice that Steane error correction fits nicely within the cluster state formalism.

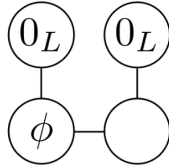
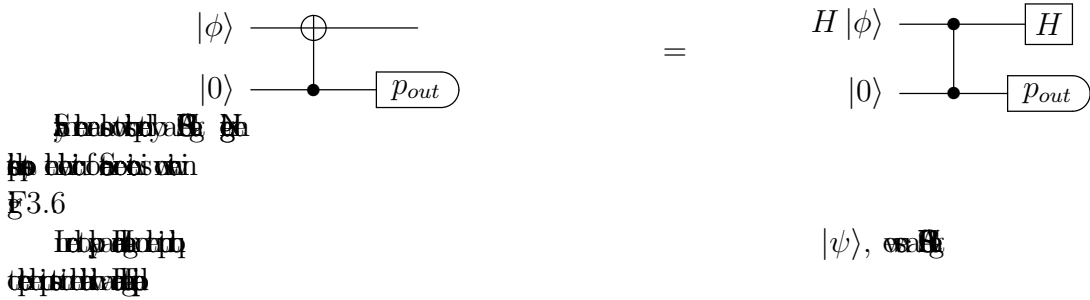
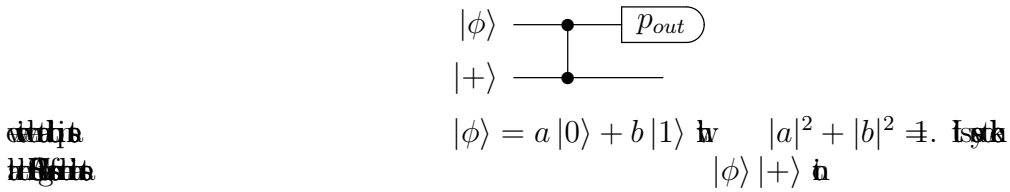


Figure 3.7: The blank node represents a \hat{p} -squeezed vacuum state, i.e. $|+\rangle$ state. All links are CPHASE gate $\hat{C}_z = e^{i\hat{q}\otimes\hat{q}}$. After measuring each of the three marked qubits in the \hat{p} quadrature, the blank node is left in state $|\phi\rangle$ with both quadratures corrected, up to a Hadamard.



Substituting Eq. 3.6 into Eq. 3.6

$|\psi\rangle$, via Eq.



with the help of

$$\begin{aligned}
 |\phi\rangle |+\rangle &\in a|0\rangle + b|1\rangle |+\rangle \\
 &\rightarrow \frac{1}{\sqrt{2}} |+\rangle (a|+\rangle + b|-\rangle) + \frac{1}{\sqrt{2}} |-\rangle (a|+\rangle - b|-\rangle)
 \end{aligned}$$

with the help of

$$\begin{aligned}
 |+\rangle &= \frac{1}{\sqrt{2}} (|0\rangle + |1\rangle) \\
 H|\phi\rangle &= a|+\rangle + b|-\rangle.
 \end{aligned}$$

with the help of Eq. 3.7

$$\begin{aligned}
 H|\phi\rangle &= a|+\rangle + b|-\rangle \\
 &= a \frac{1}{\sqrt{2}} (|0\rangle + |1\rangle) + b \frac{1}{\sqrt{2}} (|0\rangle - |1\rangle)
 \end{aligned}$$

Quantum Error Correction with continuous information

64.1 Introduction
 64.2 Continuous information
 64.3 Error correction

64.1 Introduction

64.2 Continuous information
 64.3 Error correction

64.2, Continuous information

64.3 Error correction
 64.4 Error correction

64.3 Error correction

64.4 Error correction
 64.5 Error correction

64.4, Error correction

64.5 Error correction
 64.6 Error correction

64.4 Introduction

64.4.1 Introduction

64.4.2 Introduction

64.4.3 Introduction

64.4.4 Introduction

64.4.5 Introduction

64.4.6 Introduction

64.5 Introduction

64.6 Introduction

64.7

4.1 Further Analysis of Steane Error Correction

Section 2.1.1 § 2.1.1
 This is the first part of the proof.

$$|\bar{0}\rangle \text{ in (2.10).}$$

Section 2.4 § 2.4
 This is the second part of the proof.

$$|\psi, u, v\rangle = e^{-iu\hat{p}} e^{-iv\hat{q}} |\bar{\psi}\rangle,$$

where $|\bar{\psi}\rangle$ is a state, and u, v are real numbers.

Let σ be a positive real number. Then the probability density function $P_\sigma(u)$ is given by

$$|\psi, u\rangle = e^{-iu\hat{p}} |\bar{\psi}\rangle,$$

Section 3.3, which shows that the probability of a certain event is given by the integral of the probability density function over the relevant range.

$$q_{out},$$

4.1.1 Conditional Output Errors

Section 4.1, which shows that the probability of a certain event is given by the integral of the probability density function over the relevant range.

Let $q_{out} + n\sqrt{\pi}, n \in \mathbb{Z}$. Then the probability of a certain event is given by the integral of the probability density function over the relevant range.

$$\begin{aligned} \mathbb{P}(u_1 | u_1 + u_2 = q_{out} + n\sqrt{\pi}) &= \frac{\mathbb{P}(u_1 + u_2 = q_{out} + n\sqrt{\pi} | u_1) P(u_1)}{P(u_1 + u_2 = q_{out} + n\sqrt{\pi})} \\ &= \frac{P(u_2 = q_{out} + n\sqrt{\pi} - u_1) P(u_1)}{P(u_1 + u_2 = q_{out} + n\sqrt{\pi})}. \end{aligned} \quad (4.1)$$

Let u_1 and u_2 be independent random variables with normal distributions with means μ_1 and μ_2 and variances σ_1^2 and σ_2^2 . Then the probability of a certain event is given by the integral of the probability density function over the relevant range.

$$\begin{aligned} \mathbb{P}(u_1 | u_1 + u_2 = q_{out} + n\sqrt{\pi}) &= \frac{\frac{1}{\sigma_2\sqrt{2\pi}} e^{-\frac{(u_1 - q' - l\sqrt{\pi})^2}{2\sigma_2^2}} \frac{1}{\sigma_1\sqrt{2\pi}} e^{-\frac{u_1^2}{2\sigma_1^2}}}{\frac{1}{\sqrt{\sigma_1^2 + \sigma_2^2}\sqrt{2\pi}} e^{-\frac{(q_{out} + n\sqrt{\pi})^2}{2(\sigma_1^2 + \sigma_2^2)}}} \\ &= \frac{1}{\sigma\sqrt{2\pi}} e^{-\frac{(u_1 - u_c)^2}{2\sigma^2}} \end{aligned} \quad (4.2)$$

11/11/2019

6 q_{out} is

$$\mathbb{P}(q_{\text{out}}|u_1, u_2) = \frac{1}{\mathcal{N}} \sum_{n \in \mathbb{Z}} \delta(q_{\text{out}} - u_1 - u_2 - n\sqrt{\pi}), \quad (4.5)$$

7 \mathcal{N} is

$$\mathcal{N} = \sum_{n \in \mathbb{Z}} \int_{-\frac{\sqrt{\pi}}{2}, \frac{\sqrt{\pi}}{2}] du_1 \delta(q_{\text{out}} - u_1 - u_2 - n\sqrt{\pi}) P_{\sigma_1}(u_1) P_{\sigma_2}(u_2)$$

8 $u_2 = \theta$, $q_{\text{out}} = \theta$

9 $q_{\text{out}} = \theta$

10 $q_{\text{out}} = \theta$

11 $q_{\text{out}} = \theta$

12 $q_{\text{out}} = \theta$

13 $q_{\text{out}} = \theta$

14 $q_{\text{out}} = \theta$

15 $P_{\sigma_1}(u_1) P_{\sigma_2}(u_2)$ q_{out}

$$\begin{aligned} \mathbb{P}(q_{\text{out}}) &= \int du_1 \int du_2 P_{\sigma_2}(u_2) P_{\sigma_1}(u_1) \mathbb{P}(q_{\text{out}}|u_1, u_2) \\ &= \frac{1}{\mathcal{N}} \sum_{n \in \mathbb{Z}} \int du_1 P_{\sigma_1}(u_1) P_{\sigma_2}(q_{\text{out}} - u_1 - n\sqrt{\pi}) \end{aligned} \quad (4.6)$$

16 $\int dq_{\text{out}} \mathbb{P}(q_{\text{out}}) = 1$

17 W_{succ}

$$|u_1 + u_2 - 2k\sqrt{\pi}| < \sqrt{\pi}/2$$

18 k is the number of successes

19 W_{succ}

$$e^{iq_{\text{out}} \cdot \hat{p}_1}$$

20 $u_2 \in W$

21 $|u_1 + u_2 - 2k\sqrt{\pi}| < \sqrt{\pi}/2$ $u_1, u_2 \in I_{\text{success}}$

22 W_{succ}

$$u_1, u_2 \in I_{\text{success}} \quad q_{\text{out}} = \theta$$

$$\mathbb{P}(u_1, u_2|q_{\text{out}}) = \frac{\mathbb{P}(q_{\text{out}}|u_1, u_2) P_{\sigma_1}(u_1) P_{\sigma_2}(u_2)}{\mathbb{P}(q_{\text{out}})}. \quad (4.7)$$

23 W_{succ}

$$\mathbb{P}(W_{\text{succ}}|q_{\text{out}}) = \int_{I_{\text{success}}} du_2 du_1 \mathbb{P}(u_1, u_2|q_{\text{out}}) \quad (4.8)$$

24 W_{succ}

$$\mathbb{P}(W_{\text{succ}}) = \int_{I_{\text{success}}} du_2 du_1 P_{\sigma_1}(u_1) P_{\sigma_2}(u_2). \quad (4.9)$$

25 W_{succ}

26 I_{success}

27 q_{out}

28 $u_1 + u_2 = w$

29 $w = u_1 + u_2$

30 W_{succ}

31 w

32 $\sigma = \sqrt{\sigma_1^2 + \sigma_2^2}$ I_{success}

$$|w - 2k\sqrt{\pi}| < \sqrt{\pi}/2$$

33 W_{succ}

34 $\mathbb{P}(u_1, u_2|q_{\text{out}})$

$$\mathbb{P}(w|q_{\text{out}}) = P_{\sigma}(w) \frac{\sum_{n \in \mathbb{Z}} \delta(q_{\text{out}} - w - n\sqrt{\pi})}{\sum_{n \in \mathbb{Z}} P_{\sigma}(q_{\text{out}} - n\sqrt{\pi})}. \quad (4.10)$$

So

$$\begin{aligned}
 \mathbb{P}(s \mid q_{\text{out}}) &= \int_{I_{\text{success}}} dw \mathbb{P}(w \mid q_{\text{out}}) \\
 &= \frac{1}{\sum_{n \in \mathbb{Z}} P_{\sigma}(q_{\text{out}} - n\sqrt{\pi})} \int_{I_{\text{success}}} dw P_{\sigma}(w) \sum_{n \in \mathbb{Z}} \delta(q_{\text{out}} - w - n\sqrt{\pi}) \quad (4.11) \\
 &= \frac{\sum_{n \in \mathbb{Z}} P_{\sigma}(q_{\text{out}} - n\sqrt{\pi}) f_{\text{success}}(n, q_{\text{out}})}{\sum_{n \in \mathbb{Z}} P_{\sigma}(q_{\text{out}} - n\sqrt{\pi})}.
 \end{aligned}$$

by $f_{\text{success}}(n, q_{\text{out}}) \equiv \mathbb{P}(q_{\text{out}} - n\sqrt{\pi} \in I_{\text{success}}) = \mathbb{P}(q_{\text{out}} \in [n\sqrt{\pi} - \sqrt{\pi}/2, n\sqrt{\pi} + \sqrt{\pi}/2])$.
 In $q_{\text{out}} - n\sqrt{\pi} \in I_{\text{success}}$ we have $\mathbb{P}(q_{\text{out}} \in [n\sqrt{\pi} - \sqrt{\pi}/2, n\sqrt{\pi} + \sqrt{\pi}/2])$.
 This is $\mathbb{P}(q_{\text{out}} \in [-\sqrt{\pi}/2, \sqrt{\pi}/2])$, which is q_{cor} .
 This is f_{success} from (4.11).
 So, n, q_{out}

$$\mathbb{P}(s \mid q_{\text{out}}) = \frac{\sum_{n \in \mathbb{Z}} P_{\sigma}(q_{\text{out}} - 2n\sqrt{\pi})}{\sum_{n \in \mathbb{Z}} P_{\sigma}(q_{\text{out}} - n\sqrt{\pi})}. \quad (4.12)$$

So σ is large $|w| = |u_1 + u_2| \leq \frac{2k+1}{2}\sqrt{\pi}$, k is $q_{\text{out}} \in [-\sqrt{\pi}/2, \sqrt{\pi}/2]$ then

$$\begin{aligned}
 \mathbb{P}(q_{\text{out}}) &= \int dw_1 P_{\sigma}(w) \mathbb{P}(q_{\text{out}} \mid w) \\
 &= \frac{1}{\mathcal{N}} \sum_{n \in \mathbb{Z}} \int dw_1 P_{\sigma}(w) \delta(q_{\text{out}} - w - n\sqrt{\pi}) \quad (4.13) \\
 &\approx \frac{1}{\mathcal{N}_k} \sum_{|n| \leq k} P_{\sigma}(q_{\text{out}} - n\sqrt{\pi}).
 \end{aligned}$$

by $\mathcal{N}_k \approx \frac{2k+1}{2}\sqrt{\pi}$ $\mathbb{P}(q_{\text{out}}) \approx \frac{q_{\text{out}}}{q_{\text{out}}}$ $|w| \leq$

$$\mathbb{P}(s \mid q_{\text{out}}) \approx \frac{\sum_{|2n| \leq k} P_{\sigma}(q_{\text{out}} - 2n\sqrt{\pi})}{\sum_{|n| \leq k} P_{\sigma}(q_{\text{out}} - n\sqrt{\pi})}. \quad (4.14)$$

Post-Selection Based on Conditional Error Rates

Assume $\mathbb{P}(s) = 0$, w

So $k \geq 3$ $|w_1| \leq \frac{3}{2}\sqrt{\pi}$ in (4.14). Then

$$\mathbb{P}(s \mid q_{\text{out}}) \approx \frac{P_{\sigma}(q_{\text{out}})}{P_{\sigma}(q_{\text{out}} - \sqrt{\pi}) + P_{\sigma}(q_{\text{out}}) + P_{\sigma}(q_{\text{out}} + \sqrt{\pi})}.$$

So $\mathbb{P}(s \mid q_{\text{out}}) \approx \frac{1}{3}$ $q_{\text{out}} \in [0, \sqrt{\pi}/2]$ $\mathbb{P}(s \mid q_{\text{out}}) \approx \frac{1}{3}$ $q_{\text{out}} \in [0, \sqrt{\pi}/2]$ $\mathbb{P}(s \mid q_{\text{out}}) \approx \frac{1}{3}$ $q_{\text{out}} \in [0, \sqrt{\pi}/2]$

So $\mathbb{P}(s \mid q_{\text{out}}) \approx \frac{1}{3}$ $q_{\text{out}} \in [0, \sqrt{\pi}/2]$

So $\mathbb{P}(s \mid q_{\text{out}}) \approx \frac{1}{3}$ $q_{\text{out},i} > q_{\text{sel}}$ $q_{\text{sel}} \in [0, \sqrt{\pi}/2]$

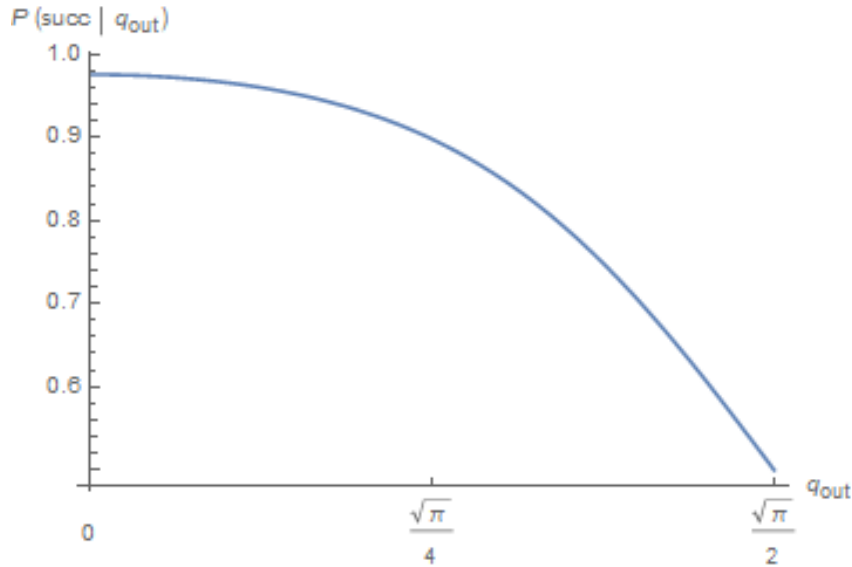


Figure 4.2: Conditional success probability with respect to measurement outcome, with the variance of the shift error $\sigma = 0.6$. The x axis is the value of the homodyne measurement outcome q_{out} , the y axis is the conditional success probability $\mathbb{P}(\text{succ}|q_{out})$, which is a monotonically decreasing function with respect to q_{out} in range $[0, \sqrt{\pi}/2]$. Note that $\mathbb{P}(\text{succ}|q_{out})$ reaches its maximum when $q_{out} = 0$, which is around 0.975.

Figure 4.2 is a plot of the conditional success probability $\mathbb{P}(\text{succ} | q_{sel})$ versus the homodyne measurement outcome q_{out} . The x-axis is labeled q_{out} and has tick marks at 0, $\frac{\sqrt{\pi}}{4}$, and $\frac{\sqrt{\pi}}{2}$. The y-axis is labeled $\mathbb{P}(\text{succ} | q_{out})$ and has tick marks from 0.6 to 1.0 in increments of 0.1. The curve starts at approximately 0.975 when $q_{out} = 0$ and decreases monotonically to 0.5 at $q_{out} = \frac{\sqrt{\pi}}{2}$. The text below the plot states: "Figure 4.2 is a plot of the conditional success probability $\mathbb{P}(\text{succ} | q_{sel})$ versus the homodyne measurement outcome q_{out} . The x-axis is labeled q_{out} and has tick marks at 0, $\frac{\sqrt{\pi}}{4}$, and $\frac{\sqrt{\pi}}{2}$. The y-axis is labeled $\mathbb{P}(\text{succ} | q_{out})$ and has tick marks from 0.6 to 1.0 in increments of 0.1. The curve starts at approximately 0.975 when $q_{out} = 0$ and decreases monotonically to 0.5 at $q_{out} = \frac{\sqrt{\pi}}{2}$. Note that $\mathbb{P}(\text{succ}|q_{out})$ reaches its maximum when $q_{out} = 0$, which is around 0.975." et. al [10]

Variance of Conditional Error Rates

From (4.14), the variance of the conditional error rate σ_{rate} is given by [10]:

$$\sigma_{rate}^2 = \int_{-\sqrt{\pi}/2}^{\sqrt{\pi}/2} dq_{out} \cdot (\mathbb{P}(\text{succ} | q_{out}) - \mathbb{P}(\text{succ}))^2 \cdot \mathbb{P}(q_{out})$$

where $\mathbb{P}(q_{out})$ is given by (4.13), and σ is the standard deviation of the shift error. For $\sigma = 0.6$, the variance of the conditional error rate is approximately 0.5, and the standard deviation is approximately 0.7.

Figure 4.3 shows the variance of the conditional error rate σ_{rate} as a function of the standard deviation of the shift error σ . The x-axis is labeled σ and has tick marks at 0.5 and 1.0. The y-axis is labeled σ_{rate} and has tick marks at 0.5 and 1.0. The curve starts at approximately 0.5 when $\sigma = 0.5$ and increases monotonically to approximately 1.0 when $\sigma = 1.0$. The text below the plot states: "Figure 4.3 shows the variance of the conditional error rate σ_{rate} as a function of the standard deviation of the shift error σ . The x-axis is labeled σ and has tick marks at 0.5 and 1.0. The y-axis is labeled σ_{rate} and has tick marks at 0.5 and 1.0. The curve starts at approximately 0.5 when $\sigma = 0.5$ and increases monotonically to approximately 1.0 when $\sigma = 1.0$. Note that σ_{rate} reaches its maximum when $\sigma = 1.0$, which is around 1.0." et. al [10]

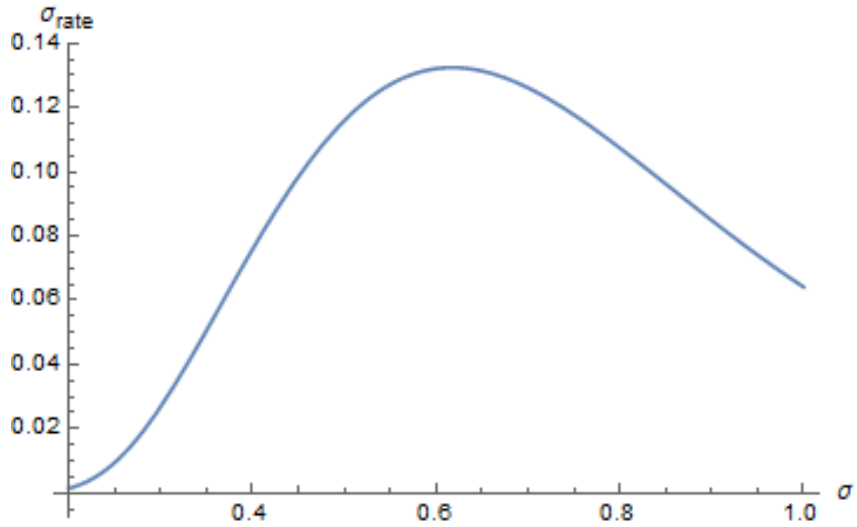


Figure 4.3: σ_{rate} is the variance of output error rates after Steane error corrections. σ is the variance of the input qubits' shift errors

4.2 Steane Error Correction with Multiple Measurements

The probability of obtaining a result q_{out} is

$$P(q_{out}) = \int_{q_{out}} \mathcal{P}(q_{out}) dq_{out}$$

The probability of obtaining a result q_{out} is

$$q_{out} = \sqrt{\pi}/2$$

The probability of obtaining a result q_{out} is

4.2.1 Double measurements in One Steane Error Correction

The probability of obtaining a result $q_{out,1}$ is

$$|\psi, u_0 + u_2, v_0 + v_1\rangle, \quad (4.4)$$

$$q_{out,1} = u_0 + u_1 + n_1\sqrt{\pi} = w_1 + n_1\sqrt{\pi} \quad (4.15)$$

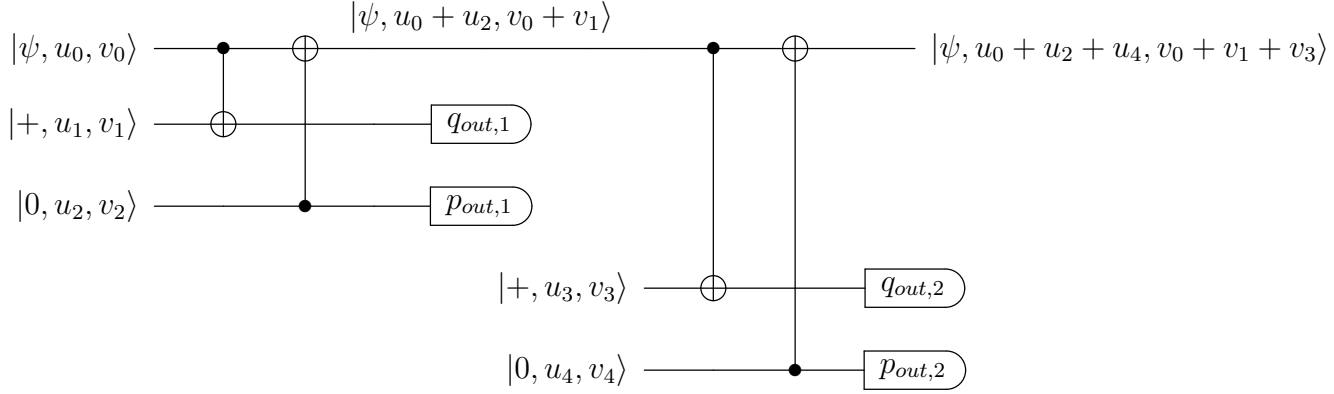


Figure 4.4: Circuit of the modified Steane error correction scheme without the correction steps. u_0 satisfy the Gaussian distribution $P_{\sigma_1}(u_0)$ with variance σ_1 . u_1, u_2, u_3, u_4 satisfy the Gaussian distribution $P_{\sigma_2}(u)$ (Here we only focus on shift errors in the \hat{q} quadrature). In order to prevent accumulating of shift errors, the measurements in the \hat{q} and the \hat{p} quadratures should be symmetric. Then this model is equivalent that we have noisy measurements, and after each measurement, there's some errors introduced. In principle this circuit could be easily generalized to more measurements.

$$w_1 = u_0 + u_1 \quad n_1 \in \mathbb{Z} \quad q_{out,1}$$

$$\begin{aligned} \mathbb{P}(q_{out,1}|w_1) &= \mathbb{P}(q_{out,1}|u_0, u_1) = \frac{1}{\mathcal{N}} \sum_{n_1 \in \mathbb{Z}} \delta(q_{out} - u_0 - u_1 - n_1\sqrt{\pi}) \\ &= \frac{1}{\mathcal{N}} \sum_{n_1 \in \mathbb{Z}} \delta(q_{out} - w_1 - n_1\sqrt{\pi}). \end{aligned} \quad (4.16)$$

$$\mathbb{P}(q_{out,1}) = \int du_0 \int du_1 P_{\sigma_1}(u_0) P_{\sigma_2}(u_1) \mathbb{P}(q_{out}|u_0, u_1) \quad (4.17)$$

$$|u_0 + u_1 - 2k\sqrt{\pi}| < \sqrt{\pi}/2 \quad k \in \mathbb{Z} \quad e^{-iq_{cor} \cdot \hat{p}_1} \quad u_0, u_1 \in I_{success}$$

$$\mathbb{P}(u_0, u_1|q_{out}) = \frac{\mathbb{P}(q_{out}|u_1, u_2) P_{\sigma_1}(u_1) P_{\sigma_2}(u_2)}{\mathbb{P}(q_{out})} \quad (4.18)$$

$$\mathbb{P}(u_0, u_1|q_{out,1}) = \int_{I_{success}} du_0 du_1 \mathbb{P}(u_0, u_1|q_{out,1}) \quad (4.19)$$

$$|q_{out,1}| \approx \frac{2k+1}{2} \sqrt{\pi} \quad k \in \mathbb{Z}$$

Figure 4.5,

$[-\sqrt{\pi}/2, \sqrt{\pi}/2)$. $n_1, n_2 \in \{0, \pm 1, \pm 2, \dots, \pm k\}$ and $|w_1|, |w_2| \leq \frac{2k+1}{2}\sqrt{\pi}$.

$$\begin{aligned} q_{out,1} &= u_0 + u_1 + n_1\sqrt{\pi} = w_1 + n_1\sqrt{\pi} \\ q_{out,2} &= u_0 + u_2 + u_3 + n_2\sqrt{\pi} = w_2 + n_2\sqrt{\pi} \end{aligned} \quad (4.25)$$

n_2 is independent of n_1 . The joint probability density function is given by

$$e^{iq_{out,2}\hat{p}}, \quad u_4 - u_3 \text{ for } n_2 \text{ and } n_1.$$

$$\begin{aligned} \mathbb{P}_1 &= \sum_{|2n| \leq k} \sum_{|n_1| \leq k} \mathbb{P}(n_1, n_2 = n | q_{out,1}, q_{out,2}), \\ \mathbb{P}_2 &= \sum_{|2n+1| \leq k} \sum_{|n_1| \leq k} \mathbb{P}(n_1, n_2 = n + 1 | q_{out,1}, q_{out,2}). \end{aligned}$$

$\mathbb{P}_1 \geq \mathbb{P}_2$ when n_2 is independent of n_1 . $e^{iq_{out,2}\hat{p}}$, $e^{i(q_{out,2} + \sqrt{\pi})\hat{p}}$.

Numerical Simulation

Let $k = 1$. Fix $n_1, n_2 \in \{0, \pm 1\}$. $|w_1|, |w_2| \leq \frac{2k+1}{2}\sqrt{\pi}$, $q_{out,1} \in [-\sqrt{\pi}/2, \sqrt{\pi}/2)$ and $q_{out,2} \in [-\sqrt{\pi}/2, \sqrt{\pi}/2)$. u_0 and u_1 are independent and $u_0 + u_1 = q_{out,1} + n_1\sqrt{\pi}$. σ_1 and σ_2 are

$$u_0 \sim \mathcal{N}\left(\frac{\sigma_1^2}{\sigma_1^2 + \sigma_2^2}(q_{out} + n_1\sqrt{\pi}), \sigma\right) \quad (4.26)$$

$$u_1 \sim \mathcal{N}\left(\frac{\sigma_2^2}{\sigma_1^2 + \sigma_2^2}(q_{out} + n_1\sqrt{\pi}), \sigma\right) \quad (4.27)$$

$\sigma^2 = \frac{\sigma_1^2\sigma_2^2}{\sigma_1^2 + \sigma_2^2}$. u_0 and u_1 are independent and $u_0 + u_1 = q_{out,1} + n_1\sqrt{\pi}$. $n_1 = -1, 0, +1$.

u_0 and u_1 are independent and $u_0 + u_1 = q_{out,1} + n_1\sqrt{\pi}$. u_2, u_3 are independent and $u_2 + u_3 = q_{out,2} + n_2\sqrt{\pi}$. $w_2 = u_0 + u_1 + u_2$ and $q_{out,2} = w_2 + n_2\sqrt{\pi}$.

$q_{out,1} \in [-\sqrt{\pi}/2, \sqrt{\pi}/2)$. \mathbb{P}_1 and \mathbb{P}_2 are n_2 is independent of n_1 .

$q_{out,1} \in [0, \sqrt{\pi}/2)$. $\mathbb{P}(n_1 | q_{out,1})$ is given by (4.5). $\mathbb{P}(n_2 | q_{out,1})$ is given by (4.5).

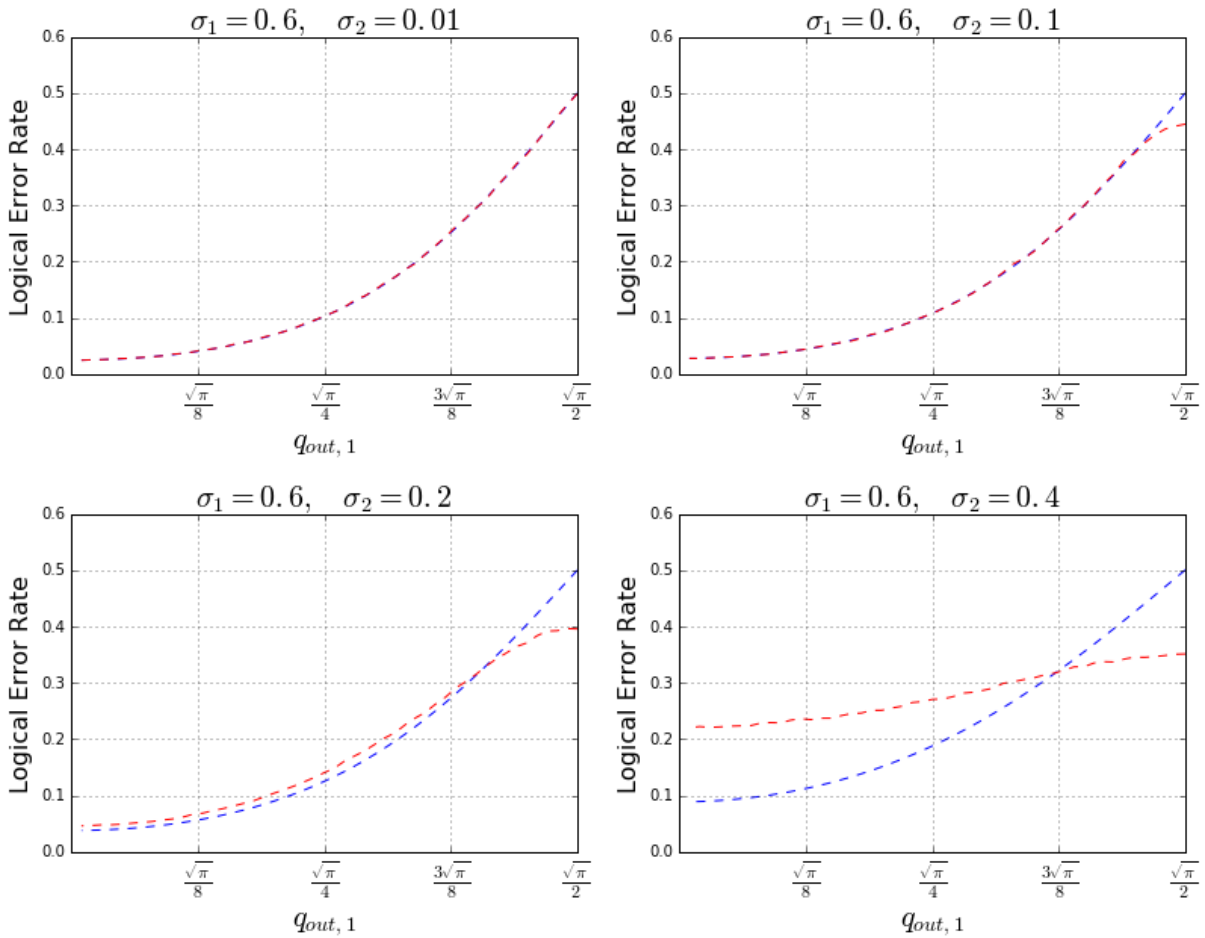


Figure 4.5: The x axis is the first measurement outcome $q_{out,1}$, the y axis is the logical error rate. The blue dashed line represents the conditional error rate $\mathbb{P}(\bar{X}|q_{out,1})$ depending on $q_{out,1}$. With this fixed $q_{out,1}$, the red dashed line represents the average logical error rate if we do a second measurement. It's clear that only when the first measurement outcome is quite close to $\frac{\sqrt{\pi}}{2}$, the second measurement can decrease the logical error rate.

Discussion

Fig 4.5, ~~table~~

to $\frac{\sqrt{\pi}}{2}$. ~~log~~

~~high~~

~~low~~

~~low~~

~~high~~

$q_{out,1}$ ~~is~~

4.3 Three-Qubit Bit-Flip Code with the GKP Code

\mathbb{R}^3 space with
 length 3
 error
 \mathbb{R}^3 code
 \mathbb{R}^3 code

$$\begin{aligned}
 |\bar{0}\rangle &= |0\rangle |0\rangle |0\rangle, \\
 |\bar{1}\rangle &= |1\rangle |1\rangle |1\rangle.
 \end{aligned}$$

error
 error
 error
 error

$$|\tilde{0}\rangle = (\sqrt{1-p_E}|0\rangle + \sqrt{p_E}|1\rangle) |0\rangle |0\rangle.$$

$Z_1 Z_2$
 $+1$ (1 - p_E)
 -1 (p_E)

$$\begin{aligned}
 |\bar{0}\rangle &= |0\rangle |0\rangle |0\rangle \\
 |\tilde{0}\rangle &= |1\rangle |0\rangle |0\rangle \\
 Z_2 Z_3 \\
 Z_1 Z_2 \quad Z_2 Z_3
 \end{aligned}$$

error
 error
 error

$$|+\rangle, |-\rangle \quad X_1 X_2 \quad X_2 X_3$$

4.3.1 Concatenation of the repetition code with the GKP Code

error
 error
 error
 error

$$\begin{aligned}
 q \\
 p_1, p_2, p_3.
 \end{aligned}$$

error
 P_1, P_2
 $Z_1 Z_2 = -1$ $Z_2 Z_3 = +1$

$$\begin{aligned}
 P_1 &= p_1 \cdot (1 - p_2) \cdot (1 - p_3), \\
 P_2 &= (1 - p_1) \cdot p_2 \cdot p_3.
 \end{aligned}$$

error
 error
 error
 error

$$\begin{aligned}
 P_1 &> P_2 \\
 p_1, p_2, p_3
 \end{aligned}$$

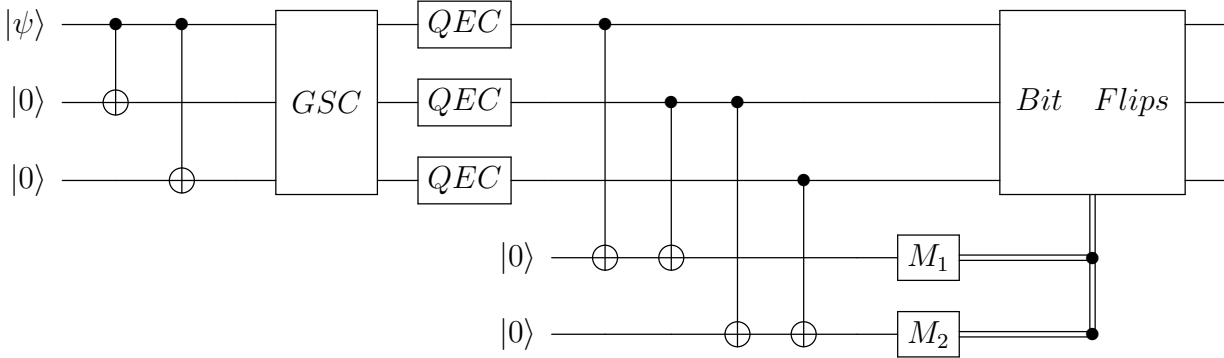


Figure 4.6: Circuit of three-qubit bit flip code [13] [5] concatenated with GKP codes. It's assumed that all GKP encoded qubits are prepared perfectly. After two CNOT gates to encode the repetition code, each qubit goes through a Gaussian shift error channel(GSC) and obtain independent gaussian shift errors in the \hat{q} quadrature with variance σ , then we do Steane error correction with ideal ancillas. Finally we measure the stabilizer checks of the bit flip code and apply the correcting operations(bit flips) according to the measurement outcomes M_1, M_2 in the \hat{q} quadrature, they corresponds to Z_1Z_2 and Z_2Z_3 respectively.

Numerical Simulation

Quantum Error Correction

and

the error rate of (4.14).

Quantum Error Correction

and

the error rate of (4.14).

Quantum Error Correction

and

the error rate of (4.14).

Quantum Error Correction

and

the

σ , and

M_1, M_2 .

P_1, P_2 for

et al. [5] and

4.4 Concatenation of the toric Code with the GKP Code

Quantum Error Correction

and

the error rate of (4.14).

Quantum Error Correction

and

the error rate of (4.14).

Quantum Error Correction

and

the error rate of (4.14).

$L \times L$ and

$$B_z = \prod_j Z_j$$

$$A_x = \prod_j X_j$$

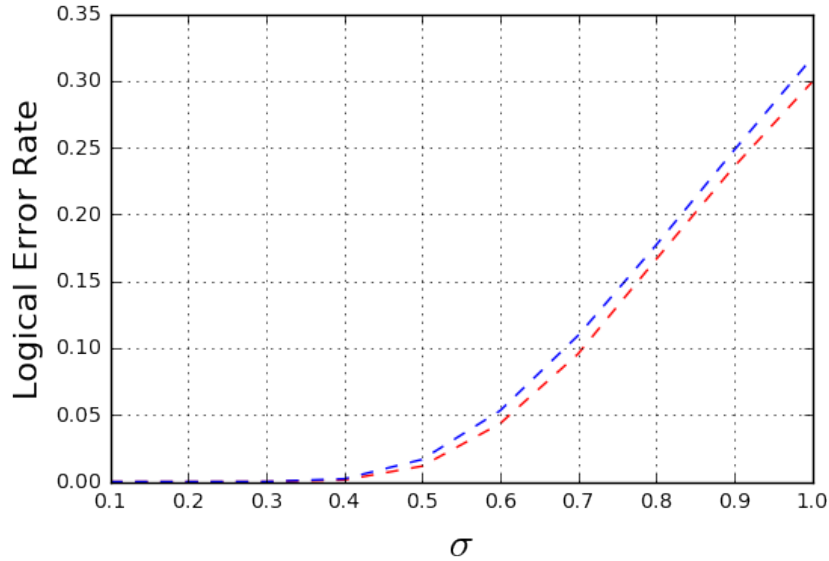


Figure 4.7: The logical error rates of correcting three-qubit bit-flip code with or without using the conditional error rates of the underlying GKP-encoded qubits. Red dashed line represents correcting with the conditional error rates. The blue dashed line represents correcting with only the average error rate. When the variance σ of the input shift error is large enough (≥ 0.4), the logical error rates can be decreased a little bit.

Decoding the Toric Code

\mathbb{F}_2
 \mathbb{F}_2
 \mathbb{F}_2
 \mathbb{F}_2
 \mathbb{F}_2

p_0
 -1

\mathbb{F}_2
 \mathbb{F}_2
 \mathbb{F}_2
 \mathbb{F}_2
 \mathbb{F}_2
 \mathbb{F}_2
 \mathbb{F}_2
 \mathbb{F}_2
 \mathbb{F}_2

\bar{X} \bar{Z}

.3% 2^7

\mathbb{F}_2
 \mathbb{F}_2
 \mathbb{F}_2
 \mathbb{F}_2

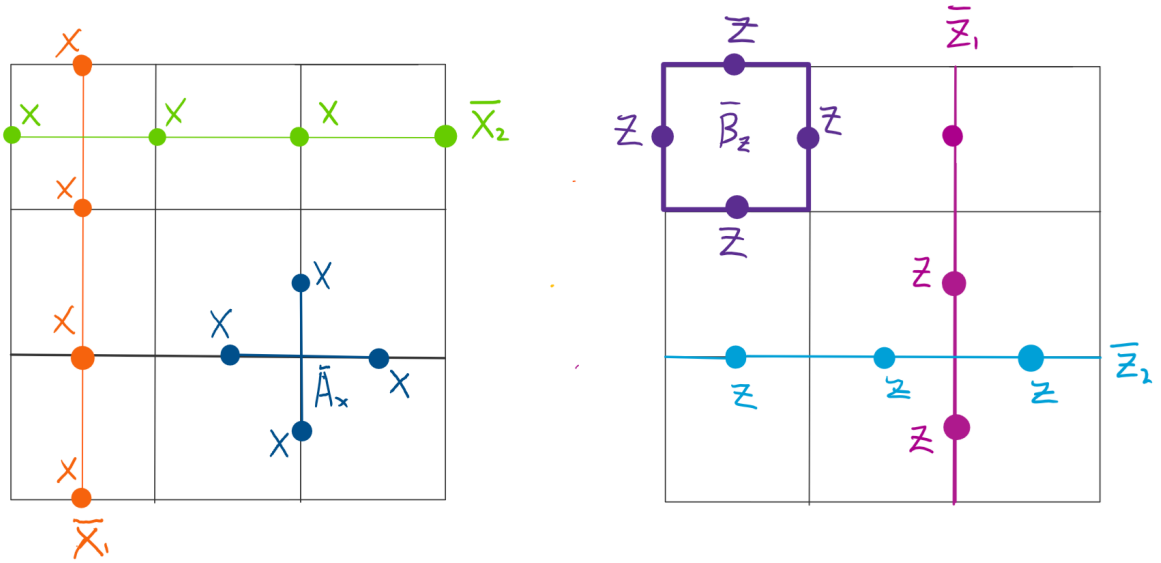


Figure 4.8: Two dimensional toric code. Where \bar{A}_x is the X check, it consists of four X operator acting on four qubits. \bar{B}_z is the Z check, it consists of four Z operator acting on four qubits. \bar{X}_i and \bar{Z}_j are logical operators of the toric code, it's easy to check they commute both stabilizers, thus they are undetectable errors. \bar{X}_i and \bar{Z}_j don't commute with each other. ($i, j = 1, 2$)

4.4.1 Only Data Qubits are Noisy

In a quantum channel

with a depolarizing

error (see

Eq. (4.13))

the

output state is given by

$$\rho_{\text{out}} = \int du_1 P_{\sigma_1}(u_1) \rho_{\text{in}} + \frac{2k+1}{2} \sqrt{\pi} \rho_{\text{in}}$$

$$\mathbb{P}(q_{\text{out}}) = \int du_1 P_{\sigma_1}(u_1) \mathbb{P}(q_{\text{out}}|u_1) \approx \frac{1}{\mathcal{N}_k} \sum_{|n| \leq k} P_{\sigma_1}(q_{\text{out}} - n\sqrt{\pi}) \quad (4.28)$$

$$\mathbb{P}(q_{\text{out}}) = \int_{I_{\text{success}}} du_1 \mathbb{P}(u_1|q_{\text{out}}) \approx \frac{\sum_{|2n| \leq k} P_{\sigma_1}(q_{\text{out}} - 2n\sqrt{\pi})}{\sum_{|n| \leq k} P_{\sigma_1}(q_{\text{out}} - n\sqrt{\pi})} \quad (4.29)$$

the probability of

success is given by

Eq. (4.13)

Eq. (4.13)

Eq. (4.13)

$$\prod_{i=1}^4 |\bar{\psi}_i\rangle \cdot |\bar{0}\rangle \rightarrow \left(\frac{1 + \prod_{i=1}^4 \bar{Z}_i}{2}\right) |\bar{\psi}\rangle \cdot |\bar{0}\rangle + \left(\frac{1 - \prod_{i=1}^4 \bar{Z}_i}{2}\right) |\bar{\psi}\rangle \cdot |\bar{1}\rangle, \quad (4.29)$$

where $|\bar{\psi}\rangle = \prod_{i=1}^4 |\bar{\psi}_i\rangle$ and \bar{Z}_i is a

logical operator

acting on

all

\bar{X}

\bar{Z} acting on $|0\rangle$,

$i = 1, 2$

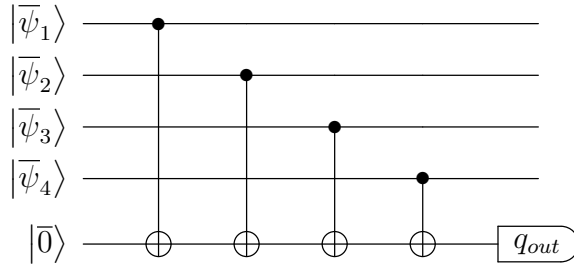


Figure 4.9: Circuit of stabilizer check $B_z = \prod_j \bar{Z}_j$. All the data qubits can only have possible logical \bar{X} errors, and ancilla is also ideal in this circuit, so the homodyne measurement outcome q_{out} can only be $n\sqrt{\pi}$, $n \in \mathbb{Z}$.

Toric Code Decoding with Message Passing

$$P(\bar{X} | q_{out,i}) = \mathbb{P}(\text{succ} | q_{out,i})$$

$$P_S = \prod_{i \notin S} (1 - \mathbb{P}(\bar{X} | q_{out,i})) \prod_{j \in S} \mathbb{P}(\bar{X} | q_{out,j}) = P_0 \prod_{j \in S} R_j \quad (4.30)$$

$$R_j = \frac{\mathbb{P}(\bar{X} | q_{out,j})}{1 - \mathbb{P}(\bar{X} | q_{out,j})} \quad P_0 = \prod_{j \in S} R_j$$

$$P_S / P_0 = \prod_{j \in S} R_j$$

$$\ln \left(\frac{P_S}{P_0} \right) = \sum_{j \in S} \ln R_j = - \sum_{j \in S} w_j \quad (4.31)$$

$$w_j = - \ln R_j = \ln \left(\frac{1 - \mathbb{P}(\bar{X} | q_{out,j})}{\mathbb{P}(\bar{X} | q_{out,j})} \right)$$

G

Numerical Simulation

σ_1

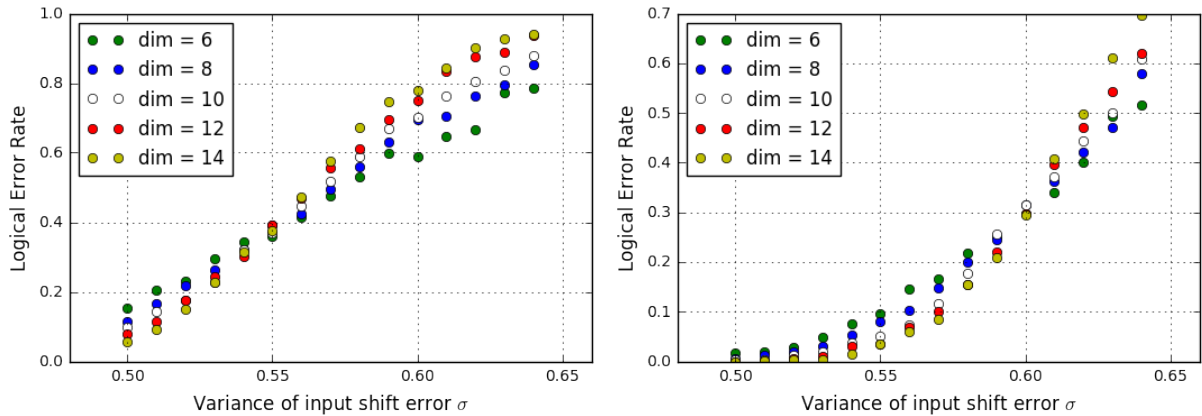


Figure 4.10: Threshold comparison between decoding with or without continuous information. On the left, the simulation only takes the average error rate into account, and we achieve the error threshold between $\sigma \approx 0.54$ and $\sigma \approx 0.55$ corresponding to $\mathbb{P}(\bar{X}) \approx 10\%$ and $\mathbb{P}(\bar{X}) \approx 10.7\%$. The threshold fits nicely with the theoretical threshold of the toric code, 10.3% [2]. On the right, the simulation takes the GKP error information (conditional error rates) into account, and the threshold is achieved with much noisier GKP states, where $\sigma \approx 0.6$ ($P(\bar{X}) \approx 14\%$). "dim" in the legends means dimension of the 2-dimensional square toric code

Figure 4.9: Threshold comparison

$$P(\bar{X}) = \sum_{q_{out,i}} P(\bar{X}|q_{out,i}) P(q_{out,i})$$

$$P(\bar{X}) = \sum_{q_{out,i}} P(\bar{X}|q_{out,i}) P(q_{out,i})$$

Figure 4.9: Threshold comparison

Figure 4.10: Threshold comparison

Figure 4.10: Threshold comparison

Figure 4.10: Threshold comparison

Figure 4.10: Threshold comparison. $\sigma \approx 0.54$ ($P(\bar{X}) \approx 10\%$) and $\sigma \approx 0.55$ ($P(\bar{X}) \approx 10.7\%$). The threshold fits nicely with the theoretical threshold of the toric code, 10.3% [2].

Figure 4.10: Threshold comparison

4.4.2 Ancilla Qubits are Also Noisy

Figure 4.10: Threshold comparison

Figure 4.10: Threshold comparison

Figure 4.10: Threshold comparison

$$\sigma_1 \text{ and } \sigma_2$$

$$u_a$$

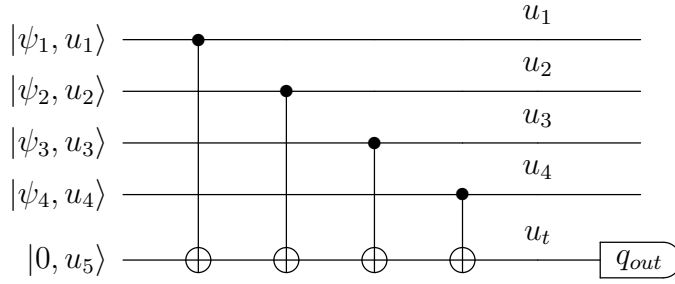


Figure 4.11: Circuit of stabilizer check $B_z = \prod_j \bar{Z}_j$. Where $u_t = \sum_{i=1}^5 u_i$ and its probability distribution is $P_{\sigma_t}(u_t)$ with $\sigma_t = \sqrt{5\sigma_2^2}$, because all the data qubits and the ancilla qubit contain a Gaussian shift error u_i with the same variance σ_2 . Also all the data qubits have an possible logical \bar{X} error. Then the homodyne measurement outcome $q_{out} = u_t + n\sqrt{\pi}$, $n \in \mathbb{Z}$. Note that q_{out} later will also be restricted that $|q_{out}| \leq \sqrt{\pi}/2$.

ca

$$\mathbb{P}(q_{out}) = \int dw P_{\sigma}(w) \mathbb{P}(q_{out}|w) \approx \frac{1}{\mathcal{N}_k} \sum_{|n| \leq k} P_{\sigma}(q_{out} - w - n\sqrt{\pi}), \quad (4.32a)$$

$$\mathbb{P}(w | q_{out}) = \int_{I_{success}} dw \mathbb{P}(w|q_{out}) \approx \frac{\sum_{|2n| \leq k} P_{\sigma}(q_{out} - 2n\sqrt{\pi})}{\sum_{|n| \leq k} P_{\sigma}(q_{out} - n\sqrt{\pi})}, \quad (4.32b)$$

bw

$$w = u_a + u_d \text{ is a shift} \quad \sigma = \sqrt{\sigma_1^2 + \sigma_2^2} \text{ dist b}$$

ph

$$|w| \leq \frac{2k+1}{2} \sqrt{\pi} \text{ dist} \quad |q_{out}| \leq \sqrt{\pi}/2. \quad \mathbb{N} \quad j = 0, 1, \dots$$

tfbis:

$$|\psi_{out}\rangle = |\psi, u_d - q_{cor}\rangle \otimes \left(-i(u_d - q_{cor}) \cdot \hat{p}_1 \right) |\bar{\psi}\rangle = e^{iu_a \cdot \hat{p}} \bar{X}^j |\bar{\psi}\rangle. \quad (4.33)$$

ca

$$q_{cor} = u_a + u_d \text{ dist} \quad \sqrt{\pi} \in [-\sqrt{\pi}, \sqrt{\pi}] \text{ dist 0.}$$

Is stabilizer check:

tfbis

$$u_a \text{ dist} \quad \bar{X} \text{ dist}$$

tfbis

$$B_z = \prod_j \bar{Z}_j \text{ dist 4.11 dist}$$

tfbis

$$|\psi, u\rangle \cdot |0, u_5\rangle \rightarrow \left(\frac{1 + \prod_{i=1}^4 \bar{Z}_i}{2} \right) |\psi, u\rangle \cdot |0, u_t\rangle + \left(\frac{1 - \prod_{i=1}^4 \bar{Z}_i}{2} \right) |\psi, u\rangle \cdot |1, u_t\rangle \quad (4.34)$$

bw

$$|\psi, u\rangle = \prod_{i=1}^4 |\psi_i, u_i\rangle \text{ dist} \quad u_t = \sum_{i=1}^5 u_i \text{ dist}$$

tfbis

$$q_{out} = u_t + n\sqrt{\pi}, \text{ dist}$$

tfbis

$$n \text{ is a } \mathbb{N} \quad n \text{ is a } \mathbb{Z}$$

tfbis

$$|0, u_t\rangle, \text{ dist} \quad B_z \text{ dist } +1. \text{ dist}$$

tfbis

$$-1 \text{ dist}$$

Is stabilizer

bw

$$u_t \text{ dist} \quad \sqrt{\pi}, \text{ ie } |u_t - 2m\sqrt{\pi}| < \sqrt{\pi}/2 \text{ dist}$$

tfbis

$$I_{success} \text{ dist}$$

is 4.1.2.

Is stabilizer

ca [2] dist

$$d \times d \text{ dist}$$

ca

is 3-1 dist

$$d \times d \times d \text{ dist}$$

is 3% dist [2]

the probability

$$u_t = \sum_{i=1}^5 u_i.$$

is

the probability

of

the

probability

of

the

probability

of

the

Correcting the Defects Conditionally

the

probability

of

the

probability

of

the

probability

of

the

probability

of

the

$$u_t = \sum_{i=1}^5 u_i \quad \text{and} \quad w = u_a + u_d$$

$$\sigma_1 \neq \sigma_2,$$

$$\mathbb{P}(\bar{X} | q_{out}).$$

$$\mathbb{P}(\bar{X}),$$

$$P_i \quad i = 1, 2, 3, 4$$

$$\bar{X}$$

$$P_{syn}$$

$$P_{syn} = 0,$$

$$P_{defect} = \sum_{i=1}^4 \left((1 - P_i) \cdot \prod_{i \neq j} P_j + P_i \cdot \prod_{i \neq j} (1 - P_j) \right). \quad (4.35)$$

the

probability

of

the

probability

$$P_{syn} > 0. \quad P_{defect} \cdot (1 - P_{syn}) - P_{defect} \cdot P_{syn}$$

$$-1$$

$$\mathbb{P}_{succ} = \frac{P_{defect} \cdot (1 - P_{syn})}{P_{defect} \cdot (1 - P_{syn}) + (1 - P_{defect}) \cdot P_{syn}}. \quad (4.36)$$

the

probability

of

the

probability

$$\mathbb{P}(\bar{X})$$

$$-1,$$

$$\bar{\mathbb{P}}_{succ} = \lim_{N \rightarrow \infty} \frac{1}{N} \sum_{i=1}^N \mathbb{P}_{succ,i},$$

the

probability

$$-1, \quad \mathbb{P}_{succ,i}$$

$$-1.$$

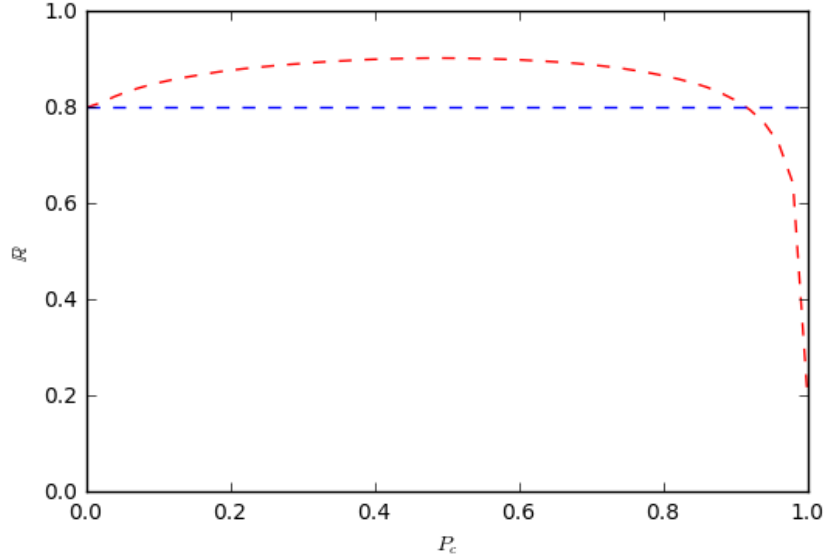


Figure 4.12: The correcting process with $\sigma_1 = 2\sigma_2 = 0.4$, $\sigma = \sqrt{\sigma_1^2 + \sigma_2^2} \approx 0.44$ and the average error rate $P(\bar{X}) \approx 4.75\%$. The x axis is the the rate P_c used as a criteria to decide whether a syndrome measurement is correct or not. Syndrome measurements will tell us that some vertices are defect, and the y axis is the ratio \mathbb{R} of the successful syndrome measurements, without the proposed correcting process it is around 80% represented by the blue line and reaches the maximum when P_c is around 0.5.

Statistics

$$\mathbb{R} = \bar{\mathbb{P}}_{succ} \quad (4.37)$$

Numerical

with 100% of the

of the

of the

of the

of

of

of the

of the

of the

of the

of the

of the

of

Numerical Simulation

with

of

of

of (4.12).

$$\sigma_1 = 2\sigma_2 = 0.4 \quad \sigma = \sqrt{\sigma_1^2 + \sigma_2^2} \approx 0.44.$$

$$P(\bar{X}) \approx 4.75\%$$

$$\mathbb{R} = \bar{\mathbb{P}}_{succ} \approx 8\%$$

4.12. D

$P_c \approx 0.5$ step

P_c th

$\mathbb{R} \approx 0\%$ in

$\mathbb{R} \approx 0\%$ step

$P(\bar{X}) \approx 2\%$ flash

2% step

$\sigma \approx 0.38 < 0.44$,

step

4.5 Beyond Minimum-Weight Matching

step

(M) step

step

step

4.5.1 Drawbacks of MWM

step

\bar{X} D \bar{Z} step

step

step

4.13, step

step 4.4.1, step

step

step

4.13, step

step

step

$Pr(A) \approx Pr(B) + Pr(C)$, step

$Pr(A) \approx Pr(B)$, D $Pr(A) \approx Pr(B)$, step

step

step

4.5.2 Maximum-Likelihood Decoder

step

et al [1] step

step

step

step

step S step A

\bar{X}, \bar{Z} step

step

step S, $\bar{X}S$, $\bar{Z}S$, $\bar{X}\bar{Z}S$, step

g_1, g_2 step

step $\bar{X}S$. step

g_1 D g_2 step

step

E step

step

step

$ES, E\bar{X}S, E\bar{Z}S, E\bar{X}\bar{Z}S$

step G step

$$\mathbb{P}(G) = \sum_{g \in G} P(g)$$

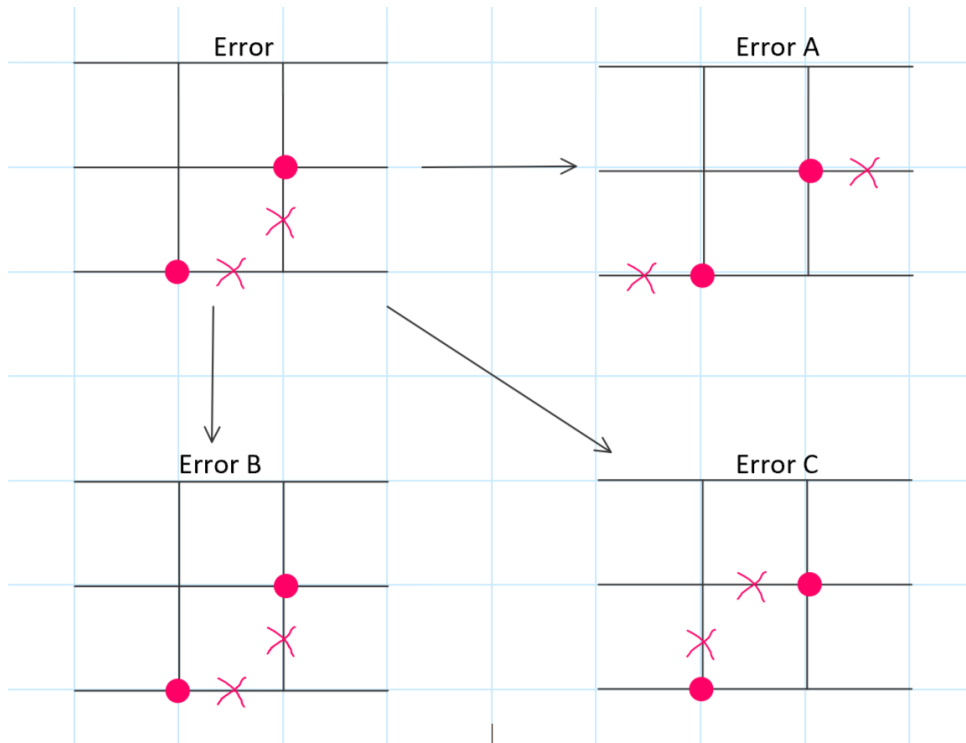


Figure 4.13: Decoding process of Minimum-Weight Perfect Matching (MWM). Error A,B,C produces the same syndromes, which fits with the actual error. MWM cannot tell the difference between them (continuous information can ameliorate this), and it's neither unable to account the equivalence of error B and C. Thus MWM is itself very likely to produce errors.

$$P(g) = \prod_i (1 - P(\bar{X}|q_{out,i})) \prod_{j \in g} P(\bar{X}|q_{out,j}) = P_0 \prod_{j \in g} R_j \quad (4.38)$$

$$R_j = \mathbb{P}(\bar{X}|q_{out,j}) / (1 - \mathbb{P}(\bar{X}|q_{out,j})) \quad P_0 = \mathbb{P}(G)$$

$$\mathbb{P}(\bar{X}|q_{out,i})$$

4.6 Discussion

§ 4.1 and § 4.2. In § 4.3 and § 4.4. It

Conclusion and Outlook

The first part of the paper discusses the importance of the research and the objectives of the study. It also outlines the structure of the paper.

In the second part, we discuss the theoretical background of the research. We start with a review of the literature on the topic. We then discuss the theoretical framework of the research. We also discuss the research methodology and the data used in the study.

In the third part, we discuss the empirical results of the study. We start with a description of the data and the variables used in the study. We then discuss the results of the regression analysis.

In the fourth part, we discuss the conclusions and the outlook of the research. We summarize the main findings of the study and discuss their implications. We also discuss the limitations of the study and suggest directions for future research.

- [13] M. A. Leigh, *Physical Review A*, **6**(2)022312, 2003.
- [14] R. DEB, H. J. B. ~~et al~~, *Physical Review A*, **6**(2)022312, 2003.
- [15] A. M. ~~et al~~, *Physical Review Letters*, **75**(9), 19
- [16] H. ~~et al~~, *Physical Review A*, **9**(1)012315, 2016
- [17] B. M. ~~et al~~, *Reviews of Modern Physics*, **8**(2)307 2015.
- [18] G. H. R. G. ~~et al~~, *Physical Review Letters*, **11**(3)030501, 2017
- [19] D. ~~et al~~, *Master Thesis, RWTH Aachen University, 2015.*
- [20] X. Z. D. W. ~~et al~~, *Physical Review A*, **0**(5)052316 2000.